Arabian Journal of Geosciences (2021) 14: 2400
https://doi.org/10.1007/s12517-021-08743-3

ORIGINAL PAPER

Provenance, tectonic setting, and source area palaeoweathering of the Lower Cretaceous Nubian sandstones at Gebel Duwi, Eastern Desert, Egypt: inferences from mineralogy and whole-rock geochemistry

Emad S. Sallam[1] · **Dmitry A. Ruban**[2]

Received: 8 August 2021 / Accepted: 26 October 2021 / Published online: 11 November 2021

Abstract
The Lower Cretaceous Nubian sandstones cover large areas in both NE Africa and Arabia. In this study, we utilized major and trace element data in combination with petrographic and heavy mineral analyses to infer the provenance model of the Nubian sandstones exposed at Gebel Duwi in the Eastern Desert of Egypt. It is established that these sandstones are mainly quartzose (quartz-arenite) and litho-quartzose deposited in fluvial and estuarine near-shore environments. The quartzose sandstones are dominantly fine to medium-grained in texture. The framework consists mainly of quartz grains (average 92.26% of rock volume), in addition to minor lithic fragments (average 4.6%), very rare feldspars (average 1.17%), and heavy mineral fractions (average 1.8%). The lithic fragments are represented mainly by siltstone and sandy siltstone, with minor lithics of gneisses. The heavy mineral assemblage comprises zircon, tourmaline, rutile (ZTR), garnet, and kyanite, with minor epidote, ilmenite, and leucoxene. Chemically, these sandstones are rich in SiO_2 and poor in CaO, MgO, K_2O, Na_2O, and P_2O_5. From trace elements, the most abundant are Ba, Th, Zr, and Sr. The provenance-related interpretations of the established rock composition imply that the Nubian sandstones were sourced mainly from a relatively proximal Paleozoic sandstones through multiple stages of fluvial recycling and were deposited in low-lying basin areas in the passive continental margin. The modal composition analysis reflects that these sandstones are mainly of cratonic interior. The ZTR-dominated heavy mineral assemblage indicates an increasing proportion of detritus recycled from older siliciclastic units of Paleozoic age. The high chemical weathering indices indicate intense subaerial weathering in a humid environment and multiple episodes of reworking, with a considerable contribution of basement denudation. A stable tectonic regime is interpreted, and intracratonic activation is not recognized.

Keywords Provenance · Tectonic setting · Palaeoweathering · Nubian sandstones · NE Africa

Introduction

Textural and compositional maturity of siliciclastic sediments depends on many factors, the most important of which are provenance, chemical weathering and alteration, duration and distance of sediment transport, sediment recycling, and diagenesis (e.g., Nesbitt and Markovics 1980; Nesbitt and Young 1982; Middelburg et al. 1988; Haughton et al. 1991; Nesbitt et al. 1996; Wanas and Abdel-Maguid 2006; Akarish and El-Gohary 2008; Zaid 2012; Zaid et al. 2015; Sallam and Wanas 2019; Wanas and Assal 2021). Mineralogical and geochemical compositions of siliciclastic sediments have been widely used to recognize sediment provenance, tectonic setting, and palaeoweathering conditions, thus

Responsible editor: Attila Ciner

✉ Emad S. Sallam
emad.salam@fsc.bu.edu.eg

Dmitry A. Ruban
ruban-d@mail.ru

[1] Department of Geology, Faculty of Science, Benha University, Farid Nada Street 15, Benha 13518, Egypt

[2] K.G. Razumovsky Moscow State University of Technologies and Management (the First Cossack University), Zemlyanoy Val Street 73, Moscow 109004, Russia

providing significant information useful in assessing palaeogeographical reconstructions and crustal evolution (e.g., Basu et al. 1975; Dickinson and Suczek 1979; Ingersoll and Suczek 1979; Bhatia 1983; Dickinson et al. 1983; Bhatia and Crook 1986; Roser and Korsch 1986, 1988; Haughton et al. 1991; Morton and Hallsworth 1994; Armstrong-Altrin et al. 2013; Löwen et al. 2018; Garzanti 2019; Garzanti and Andò 2019; Mohammedyasin and Wudie 2019; Dinis et al. 2020; He et al. 2020). Whole-rock geochemical analyses have long been applied to characterize sediment provenance linking geochemical signatures to source rocks and tectonic settings (e.g., Nesbitt and Young 1982; Dickinson et al. 1983; Haughton et al. 1991; McLennan et al. 1993; Verma and Armstrong-Altrin 2013, 2016). Numerous sophisticated methods (petrological and geochemical) and discriminant functions with their relevant diagrams were introduced by many authors interested in provenance analysis (e.g., Bhatia 1983; Dickinson et al. 1983; Bhatia and Crook 1986; Roser and Korsch 1986, 1988). A new portion of multi-dimensional diagrams for tectonic setting discrimination of siliciclastic sediments and their applications were proposed by Verma and Armstrong-Altrin (2013, 2016)).

The Red Sea Hills in eastern Egypt boast rich geological record that is crucial for deciphering the Mesozoic–Cenozoic evolution of northeastern Africa before, during, and after the separation of Arabia together with the opening of the Red Sea. Moreover, this domain is similarly crucial for understanding the sedimentary processes at the transition between interiors and periphery of a large continent. Particularly, the Cretaceous rocks in the Quseir area consist predominantly of siliciclastics, with the lowermost package comprising mainly of paralic and fluvial cross-bedded sandstones of the Nubia Formation (Ward and McDonald 1979; Ward et al. 1979; Van Houten et al. 1984; Ruban et al. 2021). This formation unconformably overlies the Precambrian basement rocks and is conformably overlain by the Quseir Formation. The thickness of the Nubia Formation is highly variable, and its age was generally assigned as Late Cretaceous (Said 1962; Guiraud et al. 2001), although some other studies indicate Early Cretaceous age (Bosworth et al. in Hamimi et al. 2020). In the present work, the Early Cretaceous Age of the Nubia Formation is followed.

The previous studies of the Nubia Formation in Egypt dealt mainly with stratigraphy and sedimentology (e.g.,

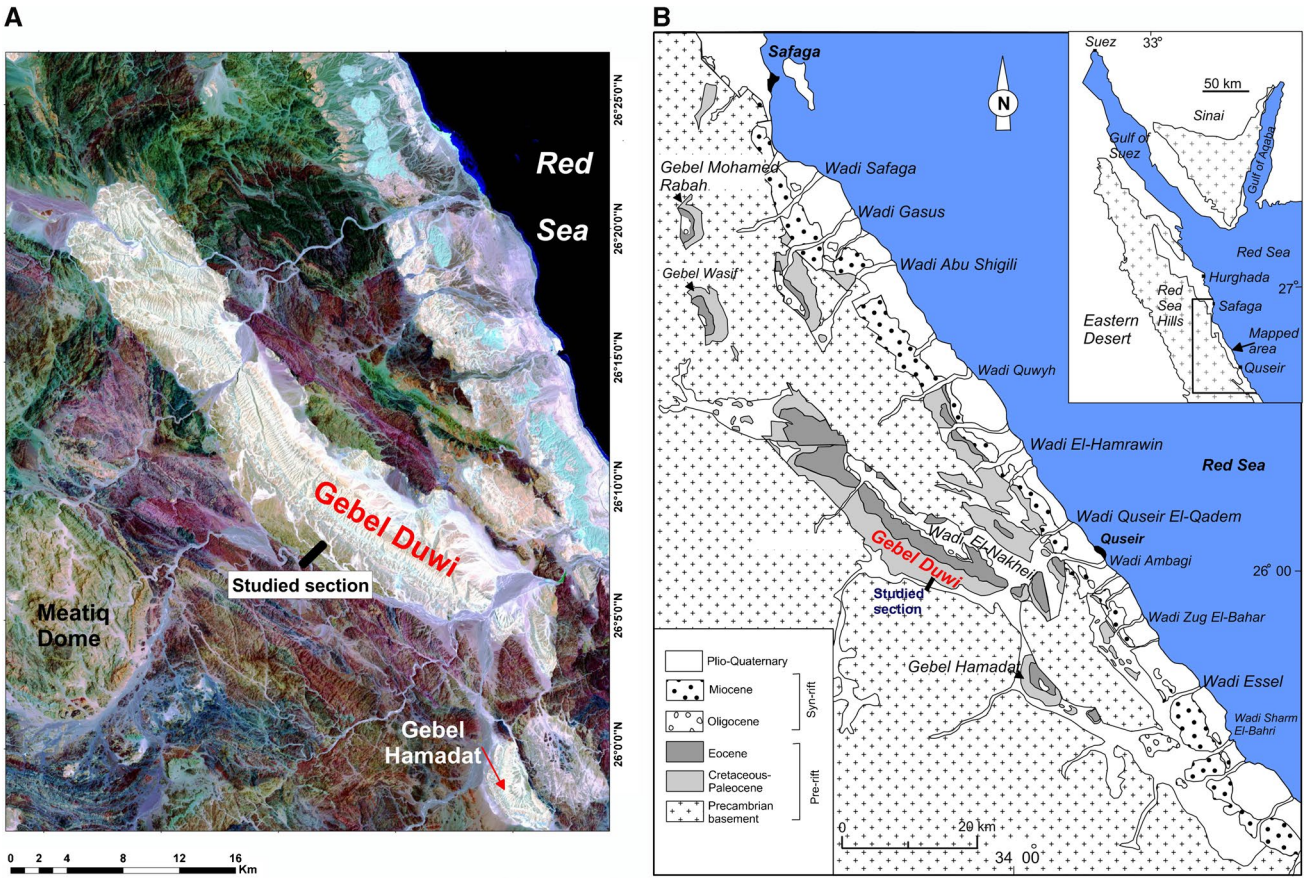

Fig. 1 **A** Landsat image showing the location of the investigated section at Gebel Duwi on the western side of the Red Sea, **B** geological map of the study area (after Youssef 1957; Khalil and McClay 2009), and **C** composite lithostratigraphic columnar section of the Mesozoic-Paleogene platform sediments in the Quseir area (after Youssef 1957)

Ward and McDonald 1979; Van Houten et al. 1984), whereas a minority of studies focused on provenance analysis of similar sandstones in neighboring countries (e.g., Weissbrod and Nachmias 1986; Amireh 1991; Kolodner et al. 2009; Ahfaf et al. 2021). Therefore, the results of petrographic and whole-rock geochemistry (major and trace elements) analyses of the Nubian sandstones at Gebel Duwi (Fig. 1) have been interpreted to clarify their provenance, tectonic setting, and source area weathering contribution, in addition to better understanding the paleogeography of northeastern Africa and Arabia in the Early Cretaceous. However, the spatial distribution of the Nubia Formation is much wider, and, thus, similar attention should be paid to composition and provenance of the relevant sandstones in many other areas of northeastern Africa and Arabia. Of special interest is how their deposition was controlled by major shoreline shifts and palaeoclimate changes on the regional scale.

Geological setting

Geographically, the study area belongs to the Central Eastern Desert of Egypt where the chain of Red Sea hills separates the internal part of northeastern Africa from the periphery of the Red Sea. More specifically, the study area

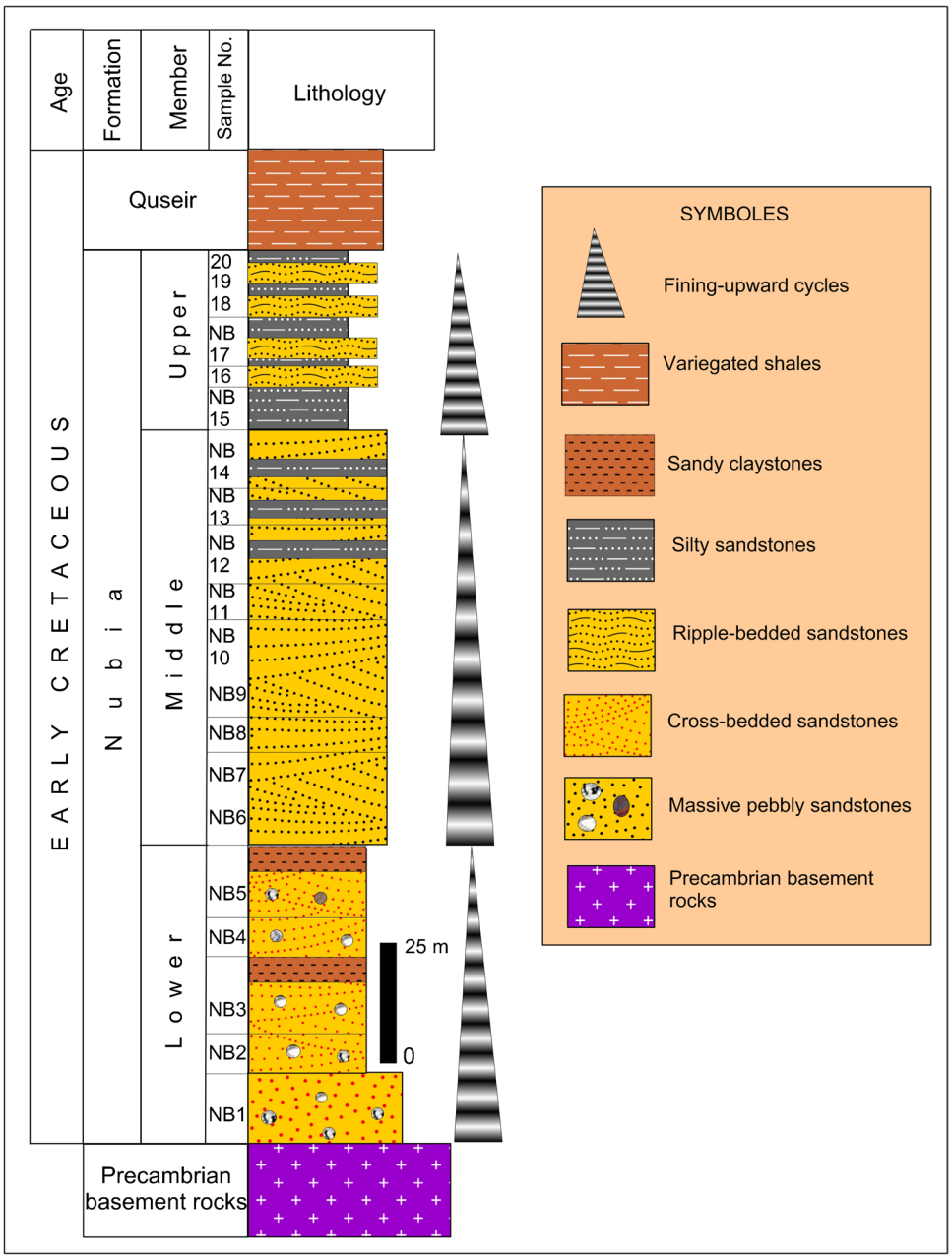

Fig. 2 Detailed lithostratigraphy of the Nubia Formation at Gebel Duwi, Quseir area

corresponds to Gebel Duwi. Tectonically, the study area is related to two main extensional fault systems and a number of half-graben basins (Khalil and McClay 2009). The junction of fault segments forms a zigzag fault pattern and rhomboidal blocks (Khalil and McClay 2009). The tectonic re-organizations linked to the Red Sea rifting led to rotation of some blocks; as a result, both pre- and syn-rift sedimentary sequences are exposed (Khalil and McClay 2009) (Fig. 1).

The pre-rift sequences (Precambrian–early Eocene) start with highly deformed volcaniclastics that were metamorphosed into the greenschist facies (Akaad and Noweir 1980; Stern 1981, 1994; Stoeser and Camp 1985; Kröner 1984, 1993). These basement rocks are unconformably overlain by a 500–700-m-thick sedimentary succession of Cretaceous–early Eocene strata. These are visible in outcrops in the Safaga–Quseir area (e.g., Gebel Duwi, Gebel Atshan, Gebel Hamadat, Gebel Mohamed Rabah, and Gebel Wasif). Particularly, the ~180-m-thick sandstones of the Nubia Formation unconformably overlie basement rocks, and these sandstones are overlain by ~70-m-thick variegated shales. The latter were separated by Youssef (1957) as a distinct stratigraphical unit of Campanian age. The upper strata include the Duwi Formation overlain by ~300 m of interbedded shales and limestones of the Upper Cretaceous–Paleocene Dakhla, Tarawan, and Esna formations (Youssef 1957; Abd El-Razik 1967; Said 1990, 2017). The youngest pre-rift unit comprises ~200-m-thick cherty limestones of the Thebes Formation.

The oldest syn-rift sequences include chert-cobble conglomerates and grits of the late Oligocene Nakheil Formation (Said 1990). It is overlain by reefal limestones, clastics, and evaporites of the Ranga, Um Mahara, Abu Dabbab, and Um Gheig formations (Philobbos et al. 1993; Said 1990). The Late Miocene–Quaternary sequences reach 1000 m in thickness offshore (Orszag-Sperber et al. 1998; Heath et al. 1999). These are marine sandstones, conglomerates, and reefal limestones of the Mersa Alam Formation and conglomerates, reefal limestones, and coarse sands of the Samadi Formation.

Sampling and methods

In this study, a multi-method approach of modal analysis, petrography, and whole-rock geochemistry has been performed to infer the provenance, depositional tectonic setting, and source area palaeoweathering of the Cretaceous

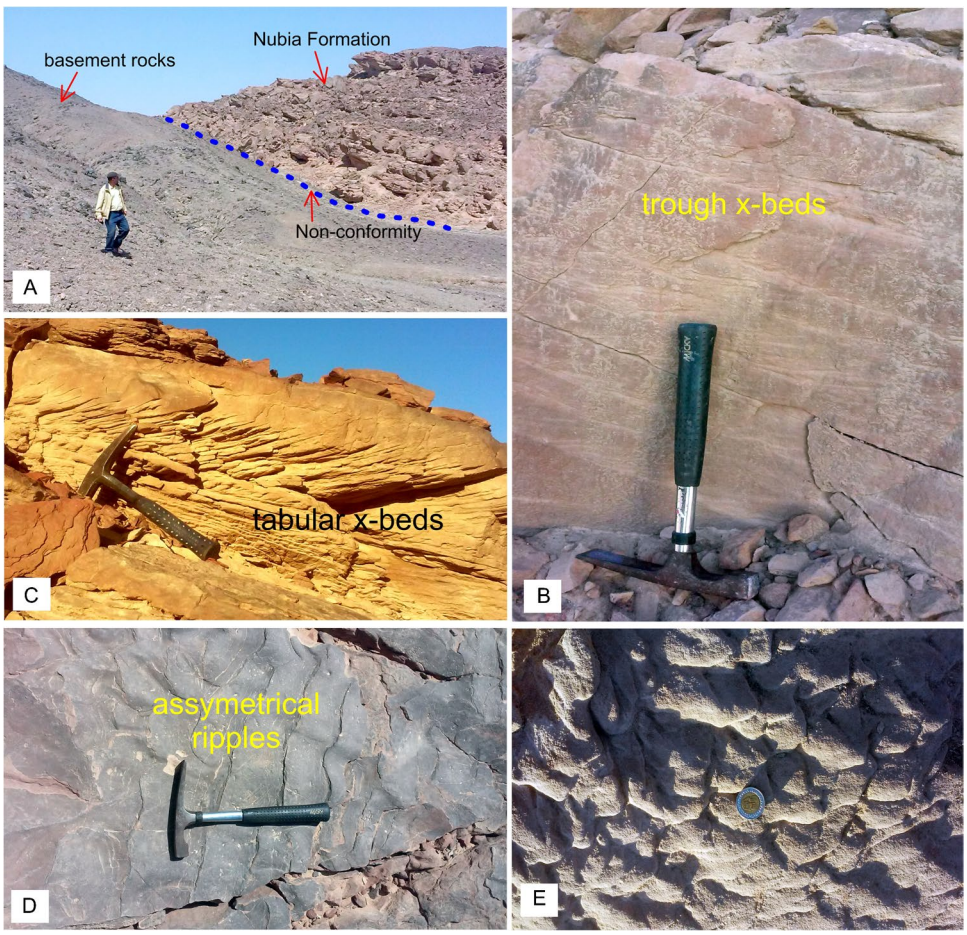

Fig. 3 Field photographs of the Nubia Formation showing **A** non-conformable contact between the Precambrian basement rocks and the overlying Nubia Formation at Gebel Duwi. Person for scale 165 cm long, **B** trough cross-bedded sandstones at the lower lithofacies of the Nubia Formation. The hammer handle for scale is 26 cm long, **C** tabular planar cross-bedded sandstones at the middle lithofacies of the Nubia Formation with a paleoflow direction to the southwest, and **D**, **E** rippled-sandstones characterizing of the upper lithofacies type of the Nubia Formation. The hammer handle for scale is 26 cm long, and coin is 2.4 cm in diameter. All photographs are made at Gebel Duwi, Quseir area

sandstones in the Red Sea Hills. One representative section of the Nubia Formation was measured, described, and sampled. The locality is Gebel Duwi—a conspicuous mountain consisting of a long sharp ridge, which drops precipitously to the southwest and slopes gently to the northeast. Its geological setting is demonstrated in Fig. 1.

A total of 65 sandstone samples were collected from the studied Nubian sandstones at Gebel Duwi (Quseir area, Eastern Desert). For the purposes of petrographic analysis, 45 thin sections of the sandstones were investigated under the standard polarizing microscope. Description of sandstone followed the classification scheme of Garzanti (2016) and Garzanti et al. (2018). Approximately 250–300 grains were counted per thin section following the traditional methodology of Gazzi-Dickinson (Ingersoll et al. 1984) for the detrital constituents (quartz, feldspars, and lithic fragments) of each studied sample. The results of modal composition analysis were tabulated and plotted in QFL ternary diagrams of Dickinson et al. (1983).

Fine to medium-grained sandstones (250–65 μm) were subjected to heavy mineral separation using bromoform (specific gravity 2.89 gm/cm^3). Then, the heavy mineral fractions were dried and mounted on a glass slide for microscopic investigation. Some of opaque and non-opaque heavy mineral fractions have been identified in the studied samples.

The samples from the Nubian sandstones were analyzed for major and trace element geochemistry using the X-ray fluorescence (XRF) spectrophotometry technique on fused and pressed beads, respectively. Analytical precision was better than 5% for major oxides and trace elements. Loss of ignition (LOI) was estimated by heating the dried sample at 1000 °C for 2 h. Major element data were recalculated to an anhydrous (LOI-free) basis and adjusted to 100% before using

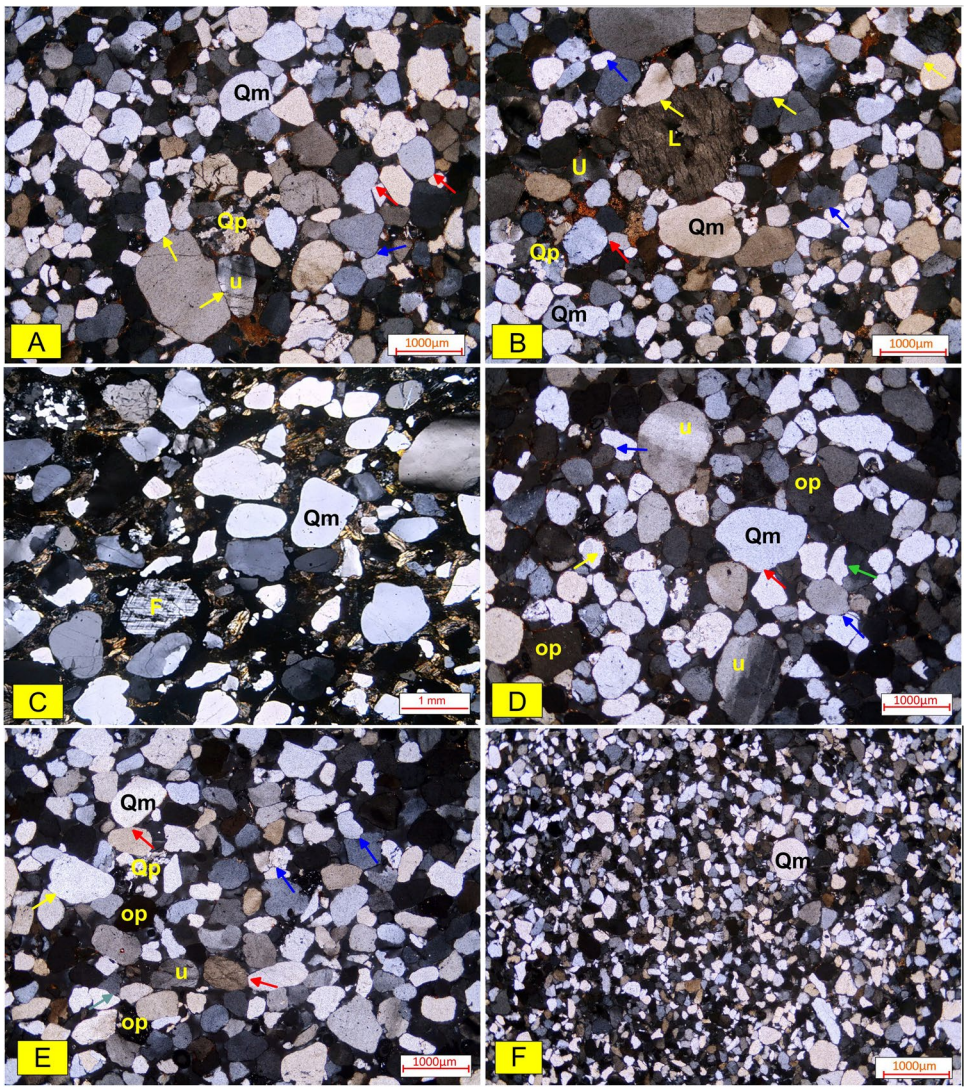

Fig. 4 Photomicrographs showing the detrital constituents of the studied sandstones: **A–E** quartz-arenites from the lower and middle lithofacies of the Nubia Formation (samples # 1, 4, 6, 7, 11, respectively), **F** fine-grained silty sandstones from the upper lithofacies of the Nubia Formation (sample # 13). Abbreviations: Qm, monocrystalline quartz; Qp, polycrystalline quartz; F, feldspars (microcline); L, lithic fragments; op, opaque minerals; u, undulose extinction, point contacts (red arrows), straight contacts (yellow arrows), concavo-convex contacts (blue arrows), and sutured contacts (green arrows)

them in various diagrams. Major and trace element analyses were carried out at the Central Laboratories of the Egyptian Mineral Resources Authority (EMRA) in Cairo, Egypt.

Results

Field observation and sedimentology

In the Gebel Duwi section, the Nubia Formation unconformably overlies Precambrian basement rocks and is succeeded by the Quseir Formation (Fig. 2). The Nubia Formation consists mainly of varicolored whitish-gray, pale yellow, and reddish sandstones with few interbeds of siltstones and claystones (Fig. 2). It attains thickness of about 180 m at the studied section. Bedding is medium and small scale. The sandstones exhibit diverse sedimentary structures such as ripples, load casts, flat- and cross-bedding, and both planar and trough types on small and medium scale. They show a fining-upward cyclic pattern (each cycle is 0.5 to 1.0 m in thickness), coarser at bottom and becomes finer upward. No marine fossils were found in these sandstones.

The Nubia Formation in the studied section can be subdivided into three lithofacies types: lower, middle, and upper lithofacies. The lower lithofacies overly unconformably the basement rocks with an erosional surface in between (Fig. 3A) and is made up of about 70-m-thick non-fossiliferous, pale yellow, medium to coarse-grained, lenticular, and planar and trough cross-bedded pebbly sandstones (Fig. 3B, C). The middle lithofacies is approximately 85 m thick and is composed of reddish-brown, fine- to medium-grained sandstones. These sandstones are characterized by the common occurrence of small-scale flat-bedded and planar cross-bedding. The latter exhibits a poly-directional pattern of palaeoflow, generally towards NNW and NNE. The upper lithofacies are about 25 m thick, and it consists of dark brown to reddish brown, fine-grained sandstones, and sandy siltstones that commonly show well-developed ripple marks (Fig. 3D, E).

Overall, the Nubia Formation was deposited predominantly in fluvial and estuarine near-shore environments interrupted by flood plains (cf. Shawa and Issawi 1978; Ward and McDonald 1979; Van Houten et al. 1984).

Table 1 Modal composition (%) of the analyzed sandstone samples

Sample no	Grain size	Sorting	Rounding	Total quartz	Quartz (monocrystalline)		Quartz (polycrystalline)	Feldspars	Lithic fragments	Heavy mineral content %
					Non-undulose	Undulose				
NB1	C	PS	R-SR	89.6	85.72	6.09	8.19	1.39	7.66	1.35
NB2	C	PS	SR	89.02	88.28	6.15	5.57	0.50	8.34	2.14
NB3	C	PS	SR	91.19	85.3	8.48	6.22	1.66	3.50	3.65
NB4	M-C	PS	R-SR	90.72	85.33	8.21	6.46	1.00	6.30	1.98
NB5	M-C	PS	R-SR	89.34	84.33	10.16	5.51	1.33	8.33	1.00
NB6	M	MS	R	89.08	84.37	8.23	7.4	2.67	7.40	0.85
NB7	M	MS	SR	91.24	86.58	9.52	3.9	1.66	4.65	2.45
NB8	M	MS	R-SR	91.39	85.15	8.49	6.36	1.34	5.67	1.6
NB9	M	MS-PS	SA-SR	92.56	90.95	6.25	2.8	1.23	3.43	2.78
NB10	M-F	MS-PS	SA-SR	93.22	90.26	6.15	3.59	1.34	2.00	3.44
NB11	M	MS	SR-SR	90.07	87.27	7.37	5.36	2.27	5.74	1.92
NB12	M-F	PS	SR	93.44	87.03	6.20	6.77	1.14	4.87	0.55
NB13	F-M	WS	R-SR	92.07	88.35	8.15	3.5	1.33	6.00	0.6
NB14	M	WS	R	93.16	85.16	8.07	6.77	1.20	5.14	0.5
NB15	VF	WS	R	95.02	87.1	7.72	5.18	1.50	2.33	1.15
NB16	F	WS	SR	94.08	86.25	10.71	3.04	1.00	3.56	1.36
NB17	F-VF	MS-WS	SR-R	95.73	81.5	11.5	7.00	0.00	2.5	1.77
NB18	F	WS	SR	94.65	84.49	8.33	7.18	0.50	2.55	2.30
NB19	F	WS	R	94.31`	89.78	5.45	4.77	0.50	1.54	3.65
NB20	VF	WS	R	97.54	94.49	2.69	2.82	0.00	0.6	1.86
Average				92.26	86.88	7.97	5.41	1.17	4.6	1.8

F fine-grained, *M* medium-grained, *C* coarse-grained, *VC* very coarse-grained, *WS* well-sorted, *PS* poorly sorted, *MS* moderately sorted, *SR* sub-rounded, *SA* sub-angular, *R* rounded

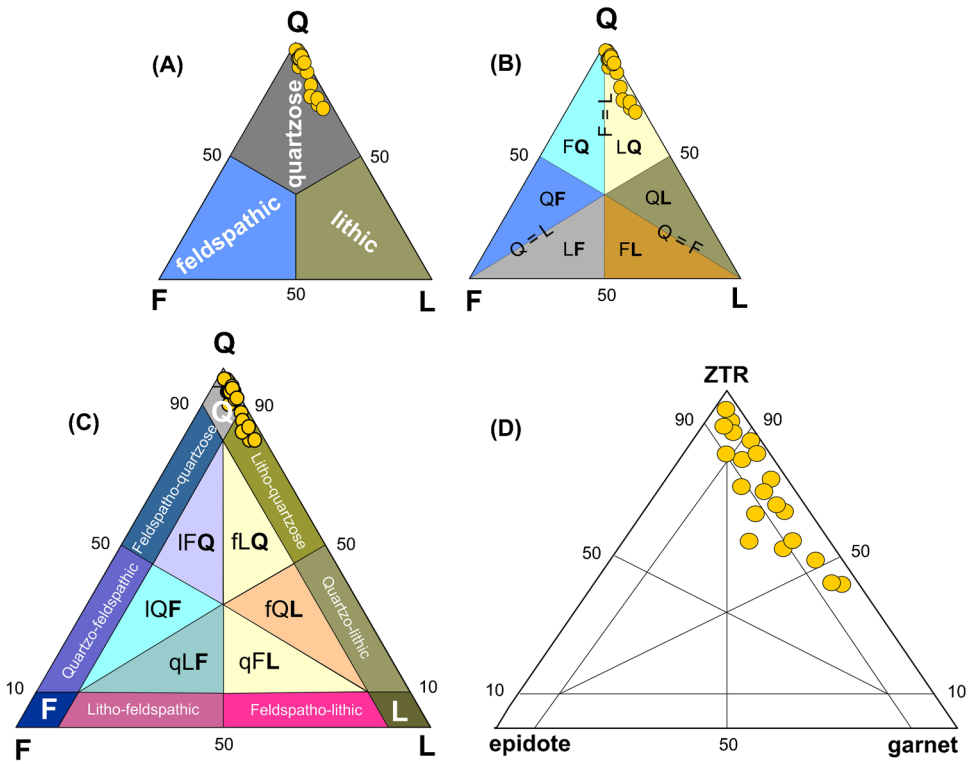

Fig. 5 **A**–**C** The QFL ternary diagram of detrital components of the studied sandstones (after Garzanti 2016 and Garzanti et al. 2018). **D** ZTR (zircon + tourmaline + rutile) versus garnet and epidote minerals. Abbreviations: Q, total quartz; F, feldspars; L, lithic fragments. Deep yellow circles represent the studied samples

Table 2 Major element geochemical data (wt. %), CIA and CIW values of the analyzed sandstone samples

Sample no	SiO_2%	TiO_2%	Al_2O_3%	Fe_2O_3%tot	MnO%	MgO%	CaO%	Na_2O%	K_2O%	P_2O_5%	LOI %	CIA	CIW
NB1	97.45	0.04	0.88	0.7	0.1	0.01	0.01	0.01	0.01	0.01	0.55	97.76	98.86
NB2	97.2	0.05	0.7	0.6	0.09	0.01	0.1	0.1	0.01	0.01	0.52	86.23	87.31
NB3	97.3	0.06	0.55	0.7	0.09	0.43	0.1	0.02	0.01	0.01	0.55	94.54	96.19
NB4	94.2	0.27	3.1	0.86	0.07	0.01	0.11	0.01	0.01	0.01	1.2	99.30	99.62
NB5	97.14	0.11	0.65	0.62	0.06	0.01	0.1	0.01	0.01	0.01	1.08	96.76	98.22
NB6	98.9	0.04	0.45	0.3	0.06	0.01	0.01	0.01	0.01	0.01	0.02	95.71	97.79
NB7	98.6	0.07	0.4	0.3	0.07	0.01	0.01	0.01	0.01	0.01	0.32	95.20	97.52
NB8	96.79	0.08	0.98	0.26	0.07	0.01	0.01	0.02	0.01	0.01	1.1	97.01	97.98
NB9	97.96	0.1	0.76	0.35	0.07	0.01	0.01	0.01	0.01	0.01	0.3	97.41	98.68
NB10	97.34	0.04	0.5	0.28	0.06	0.01	0.01	0.01	0.01	0.01	0.52	96.12	98.00
NB11	98.9	0.04	0.2	0.2	0.06	0.01	0.01	0.01	0.01	0.01	0.21	90.84	95.16
NB12	98.2	0.1	0.6	0.25	0.06	0.01	0.01	0.01	0.01	0.01	0.51	96.75	98.33
NB13	98.62	0.02	0.56	0.22	0.07	0.01	0.01	0.01	0.01	0.01	0.04	96.52	98.21
NB14	96.18	0.23	0.95	0.85	0.08	0.01	0.01	0.02	0.01	0.01	0.58	96.92	97.92
NB15	98.02	0.05	0.58	0.68	0.08	0.01	0.01	0.01	0.01	0.01	0.37	96.64	98.86
NB16	92.5	0.03	2.87	0.23	0.06	0.01	0.01	0.01	0.01	0.01	0.43	99.31	98.28
NB17	94.21	0.04	1.74	0.41	0.07	0.01	0.01	0.02	0.01	0.01	0.51	98.31	99.65
NB18	90.89	0.1	3.69	0.35	0.08	0.01	0.1	0.01	0.01	0.01	0.62	99.46	98.86
NB19	96.18	0.06	2.56	0.56	0.1	0.01	0.01	0.01	0.01	0.01	0.45	99.22	99.73
NB20	95.67	0.1	2.68	0.72	0.06	0.01	0.01	0.1	0.01	0.01	0.73	96.06	99.61
Average	96.61	0.078	1.27	0.471	0.075	0.031	0.033	0.021	0.01	0.01	--	96.30	97.62
UCC*	66.62	0.64	15.40	5.04	0.10	2.48	3.59	3.27	2.80	0.15	--	52.74	--

**UCC* upper continental crust values (after Rudnick and Gao (2003))

The common occurrence of planar cross-bedded sandstones suggests a downstream migration of transverse bars and sand waves in shallow water stream channels under lower flow regime conditions (Miall 1988; Wanas et al. 2015; Sallam et al. 2018; Ruban et al. 2019; Sallam and Ruban 2020). The siltstones and claystone interbeds represent overbank (floodplain) sedimentation. Color mottling, desiccation cracks, and red coloration indicate that these floodplain deposits were subaerially exposed and underwent pedogenesis and soil formation (Issawi et al. 2005; Sallam et al. 2015; Wanas et al. 2015). The upper part of the Nubia Formation consists mainly of paralic and deltaic sediments, which gradually passed up into shallow-marine sediments (variegated shales and glauconitic sandstones) of the overlying Quseir Formation (Ward and McDonald 1979). Gradational contact between the Nubia Formation and the overlying Quseir Formation is noticed.

Petrography, heavy mineral fractions, and modal composition

The petrographic investigation of the studied sandstones revealed that the framework composition of sediments is largely quartz-dominated (average 92.26% of the rock volume), subordinate lithic fragments (average 4.6% of the rock volume and are represented mainly by siltstones and sandy siltstones), and minor proportions of feldspars (mainly microcline) and heavy fractions (Fig. 4A–F). Feldspars and heavy fractions constitute more or less 2% of the rock volume. The sandstones are fine to medium-grained and moderately well-sorted. The matrix is chiefly composed of silt-grade quartz. The cement material is commonly ferruginous and quartz overgrowths. The pores are intergranular and irregular in shape, and they are relatively connected. Modal composition analysis (quartz–feldspars–lithic fragments, QFL) of the analyzed samples showed that the Nubian sandstones have average proportions of $Q_{92.2}F_{1.1}L_{4.6}$ (Table 1). In the QFL ternary diagrams of Garzanti (2016) and Garzanti et al. (2018), all examined sandstone samples can be classified as quartzose and pure quartzose to litho-quartzose (Fig. 5A–C). The recognized heavy minerals mainly comprise zircon, tourmaline, rutile (high ZTR index), garnet, kyanite, in addition to minor epidote, ilmenite, and leucoxene (Fig. 5D and Fig. S-1, see supplement).

The quartz grains are sub-angular to sub-rounded and show point to straight and concavo-convex grain-to-grain contacts. Monocrystalline quartz dominates (91.8–97.2%)

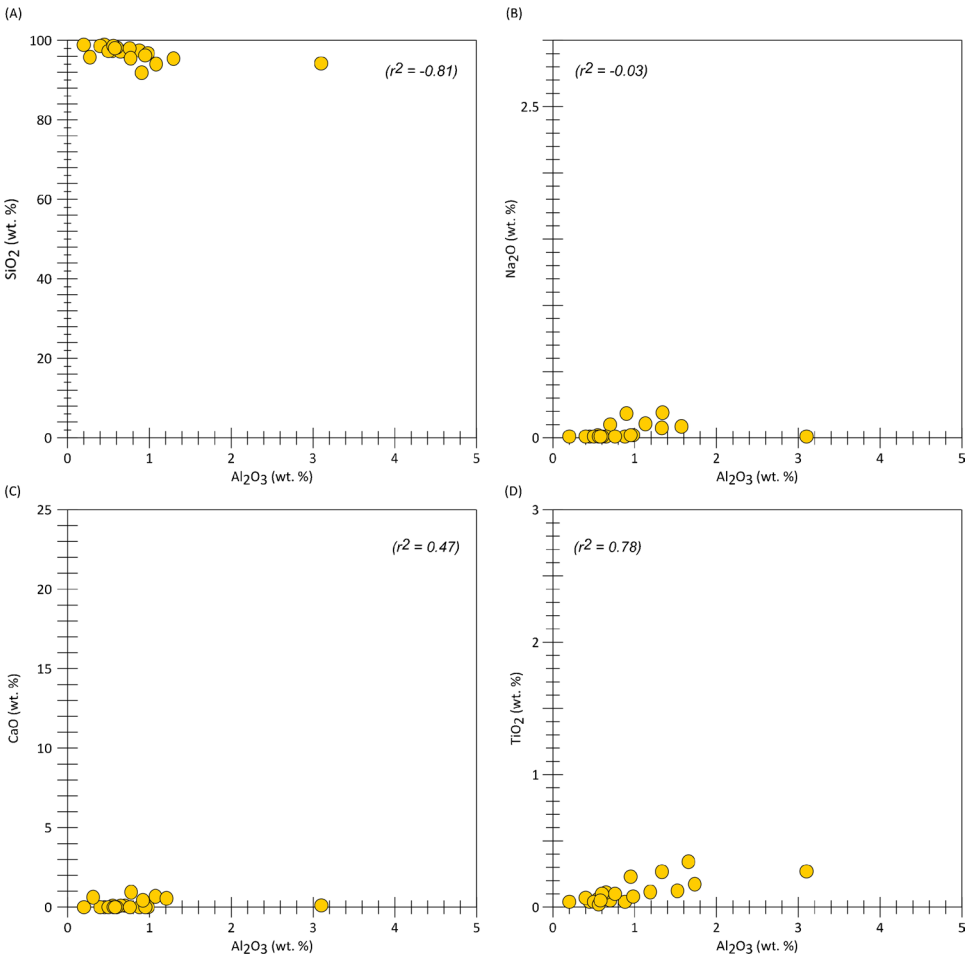

Fig. 6 **A**–**D** Correlation diagrams of Al_2O_3 with other major oxides

and shows unit (non-undulose) extinction (81.5–94.4%). A few quartz grains display slightly undulose extinction (2.6–11.5%). Polycrystalline (composite) quartz is less frequent (2.8–8.1%). The modal composition data are shown in Table 1. The main diagenetic features recognized in the investigated sandstone samples include compaction, cementation, hematitization, and quartz overgrowths. In general, the studied samples of the Nubia sandstones are chemically (compositionally) and texturally mature.

Geochemistry

Major element geochemistry

The results of major oxides of our studied samples are compared to those of the upper continental crust (UCC) (Table 2). The studied sandstone samples are enriched in SiO_2 (average 96.61%) (Table 2). In contrast, they have very low concentrations of TiO_2 (average 0.078%) and MnO (average 0.075%), and the content of CaO, MgO, K_2O, Na_2O, and P_2O_5 is also very low (Table 2). The very low percentages of K_2O and Na_2O are consistent with the scarcity of feldspar minerals. Besides, Al_2O_3 shows strong positive linear correlation with TiO_2 ($r^2 = 0.78$) and slight positive correlation with CaO ($r^2 = 0.47$), whereas it displays a strong negative linear correlation with SiO_2 ($r^2 = -0.81$) and with NaO_2 ($r^2 = -0.03$) (Fig. 6A–D).

Trace element geochemistry

The results of trace elements of our studied sandstone samples are compared to those of the upper continental crust (UCC) (Table 3). Trace element data shows a relatively high concentrations of Ba (148–244 ppm), Th (8.4–11.4 ppm), Zr (27–117 ppm), and Sr (27–117 ppm); moderate concentrations of Co (44–48 ppm) and Cu (12–18 ppm); and low concentrations of La (14–17 ppm), Ni (4–14 ppm), Zn (3–10 ppm), Nb (3–10 ppm), and Pb (5–12 ppm) (Table 3). Apparently, the enrichment in Ba, Zr, and Sr concentrations most probably reflect zircon and possibly monazite in the heavy mineral fractions. In addition, Al_2O_3 has slight positive correlations with Co ($r^2 = 0.16$), Ni ($r^2 = 0.21$), and Cu ($r^2 = 0.2$), while displaying relatively high positive correlations with Zn ($r^2 = 0.5$) (Fig. 7A–D). Plots of Fe_2O_3tot versus Co, Ni, Cu, and Zn showed slight positive correlations, with correlation coefficient (r^2) values of 0.06, 0.06, 0.3, and 0.19, respectively (Fig. 8A–D).

Concentrations of selected trace elements of the studied Nubia samples have been normalized to average upper

Table 3 Trace element geochemical data (given in ppm) of the analyzed sandstone samples

Sample No	Ba	Co	Cr	Cu	Sr	Th	La	Zn	Nb	Zr	Ni	Pb	Rb	V	Y
NB1	198.00	46.00	2.00	18.00	43	9.40	15	9	4	43	6	5	4	12.00	9.22
NB2	202.00	45.00	2.00	16.00	40	9.20	15	7	5	88	7	5	3	15.00	13.64
NB3	207.00	44.00	2.00	12.00	37	9.10	15	5	4	37	7	5	5	8.00	15.20
NB4	224.00	46.00	3.00	16.00	117	10.60	17	10	10	117	8	12	3	22.00	6.87
NB5	168.00	46.00	3.00	14.00	68	10.40	15	4	8	108	6	7	4	32.00	7.54
NB6	178.00	45.00	2.00	15.00	27	9.00	14	4	4	27	4	5	4	14.00	11.65
NB7	244.00	44.00	2.00	17.00	32	8.90	16	5	5	32	4	7	4	25.00	14.80
NB8	233.00	45.00	2.00	15.00	46	8.40	16	3	4	79	6	7	3	40.00	9.43
NB9	215.00	45.00	2.00	17.00	42	9.60	17	10	5	68	8	8	4	26.00	6.70
NB10	186.00	44.00	2.00	12.00	71	10.60	17	6	8	34	7	5	5	6.00	10.40
NB11	170.00	45.00	2.00	13.00	38	9.60	15	7	3	38	5	7	3	18.00	12.10
NB12	188.00	48.00	2.00	14.00	62	10.40	15	5	5	62	5	8	4	27.00	8.50
NB13	196.00	46.00	2.00	17.00	32	10.90	16	4	5	57	6	7	4	34.00	9.30
NB14	184.00	46.00	2.00	16.00	36	10.20	17	8	4	62	8	6	5	36.00	7.40
NB15	189.00	48.00	2.00	18.00	45	11.30	15	3	4	45	14	6	3	19.00	5.20
NB16	175.00	46.00	3.00	15.00	35	9.00	16	6	8	46	6	7	4	24.00	10.45
NB17	220.00	45.00	2.00	14.00	42	8.60	17	10	10	64	5	8	4	26.00	9.70
NB18	178.00	48.00	3.00	16.00	43	9.30	14	4	5	36	12	5	3	36.00	13.25
NB19	148.00	45.00	2.00	12.00	64	11.40	17	5	4	55	8	5	5	18.00	7.90
NB20	253.00	46.00	3.00	15.00	28	9.70	16	6	8	69	5	6	3	24.00	9.60
Average	197.80	45.65	2.25	15.1	47.4	9.78	15.75	6.05	5.65	58.35	6.85	6.55	3.85	23.1	9.94
UCC*	624	17.30	92	28	320	10.5	31	67	12	193	47	17	84	97	21

**UCC* upper continental crust values (after Rudnick and Gao (2003))

continental crust (UCC; values from Rudnick and Gao 2003). These include the large-ion lithophile easily mobilized elements (e.g., Ba, Rb, and Sr) and high-field strength immobile elements (e.g., Nb and Zr) (Fig. 9), which can reveal significant clues into sedimentary provenance (Taylor and McLennan 1985).

Discussion

Interpretation procedures

In this study, multidisciplinary methods of petrography, modal analysis, heavy mineralogy, and whole-rock geochemistry of the Nubian sandstones at Gebel Duwi have been performed to constrain their provenance, tectonic setting, source area palaeoweathering, and palaeoclimatic conditions. The present study followed the algorithm of provenance analysis based on the following established interpretation procedures.

The QFL schemes of Garzanti (2016) and Garzanti et al. (2018) and the bipyramidal diagram of Tortosa et al. (1991) are followed for provenance discrimination. The discriminant diagrams of Basu et al. (1975) and Roser and Korsch (1988) are followed for provenance characterization, whereas the tectonic setting is distinguished following the discriminant diagrams of Bhatia (1983), Dickinson et al. (1983), Roser and Korsch (1986), Kroonenberg (1994), and Verma and Armstrong-Altrin (2013, 2016)). The chemical index of weathering (CIW) and the chemical index of alteration (CIA) are used to measure the degree of source area weathering. The CIA is calculated following the equation of Nesbitt and Young (1982) as CIA = $[Al_2O_3/(Al_2O_3 + K_2O + CaO^* + Na_2O)] \times 100$. The CIW is calculated based on the equation of Harnois (1988) as CIW = $[Al_2O_3/(Al_2O_3 + CaO^* + Na_2O)] \times 100$ (where CaO* is CaO content in silicate fraction: $CaO^* = CaO\text{-}(10/3) \times P_2O_5$).

Provenance

In this study, the provenance analysis of the sandstones is based mainly on both petrography and whole-rock geochemistry (major and trace elements). Petrographic characteristics of sandstones can provide significant clues for reconstructing their depositional settings especially when fossil datasets

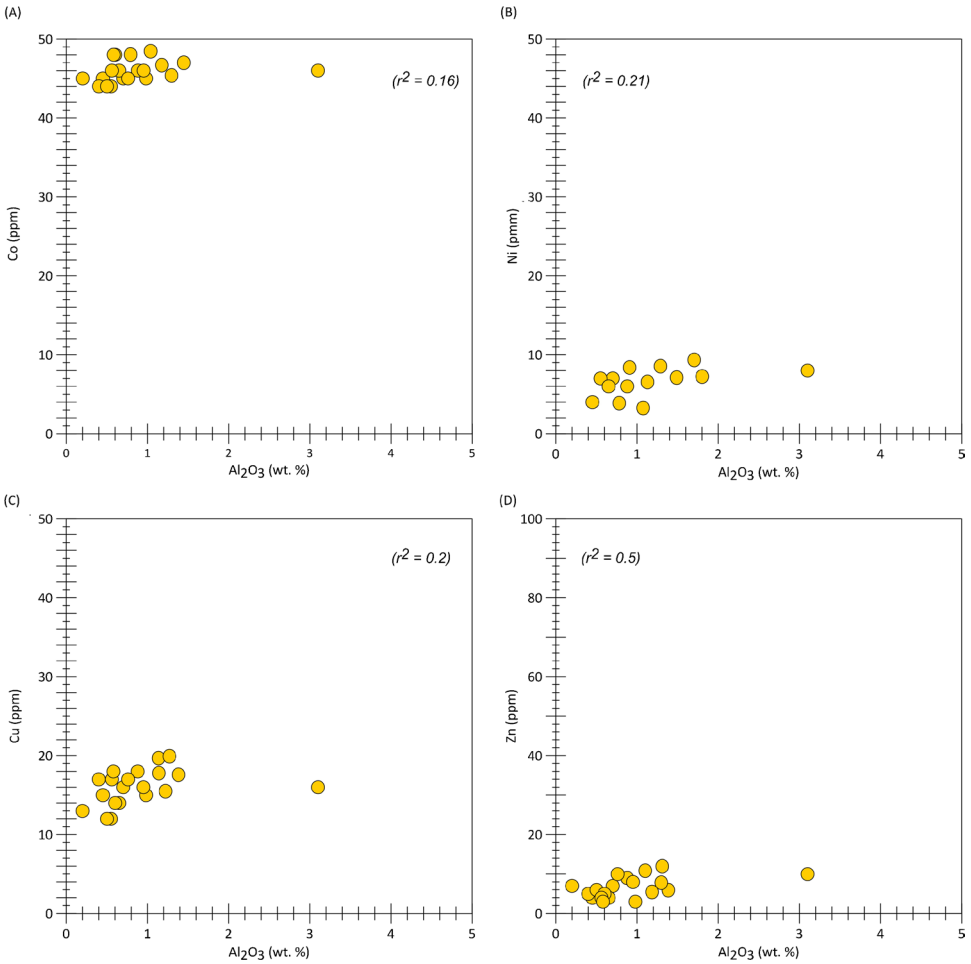

Fig. 7 **A**–**D** Correlation diagrams of Al_2O_3 with Co, Ni, Cu, and Zn

are unobtainable or inadequate (Akinlotan et al. 2021). Generally, quartzose and litho-quartzose are the most common type of sandstones in all studied samples. Due to the scarcity of feldspars in the studied sandstones, the provenance was chiefly inferred by relying only on crystallinity and extinction of quartz grains. The high quartz contents (average 92.26%) may reflect that the samples were subjected to intense periods of chemical and physical weathering and possible derivation from pre-existing sandstones (most probably multi-recycling of Paleozoic sandstones). The quartzose sandstones are generally characteristic of fluviatile sediments (cf. Kolodner et al. 2009; Ahfaf et al. 2021). Based on the bipyramidal plot diagram after Basu et al. (1975) and modified by Tortosa et al. (1991), the ratio of polycrystalline quartz grains versus undulose (strained) and non-undulose (unstrained) monocrystalline quartz grains (Table 1) indicates that quartz grains are possibly derived from plutonic igneous rocks (Fig. 10). In addition, the relative abundance of the unstrained quartz grains in the investigated sandstone samples (Table 1) points to a plutonic igneous provenance (Basu et al. 1975; Hindrix 2000).

The heavy mineral assemblage recognized from the studied sandstone samples comprising zircon and rutile might be derived from acidic igneous rocks and/or recycled older sediments (Folk 1974; Morton 1985; Kolodner et al. 2009), whereas garnet and tourmaline grains were derived likely from metamorphosed igneous rocks, especially gneisses and schists (Morton 1985; Morton and Hallsworth 1994). The ZTR-dominated assemblages beside the low plagioclase/feldspars ratio in the examined sandstone samples indicate their derivation from recycled older siliciclastic rocks. The compositional and textural maturity of the sandstones confirms the predominance of recycling processes within the basin (Wanas and Assal 2021).

The discrimination function diagram after Roser and Korsch (1988) indicates that the studied sandstones were sourced from polycyclic older quartzose sandstones (Fig. 11). Different proxies such as Al_2O_3 versus TiO_2 and Zr versus TiO_2 cross plots after Hayashi et al. (1997), Y/Ni versus Cr/V cross plot after Hiscott (1984), and Ni versus Cr cross plot after Garver et al. (1996) indicate mixed felsic and mafic source rocks of the upper continental crust (UCC)

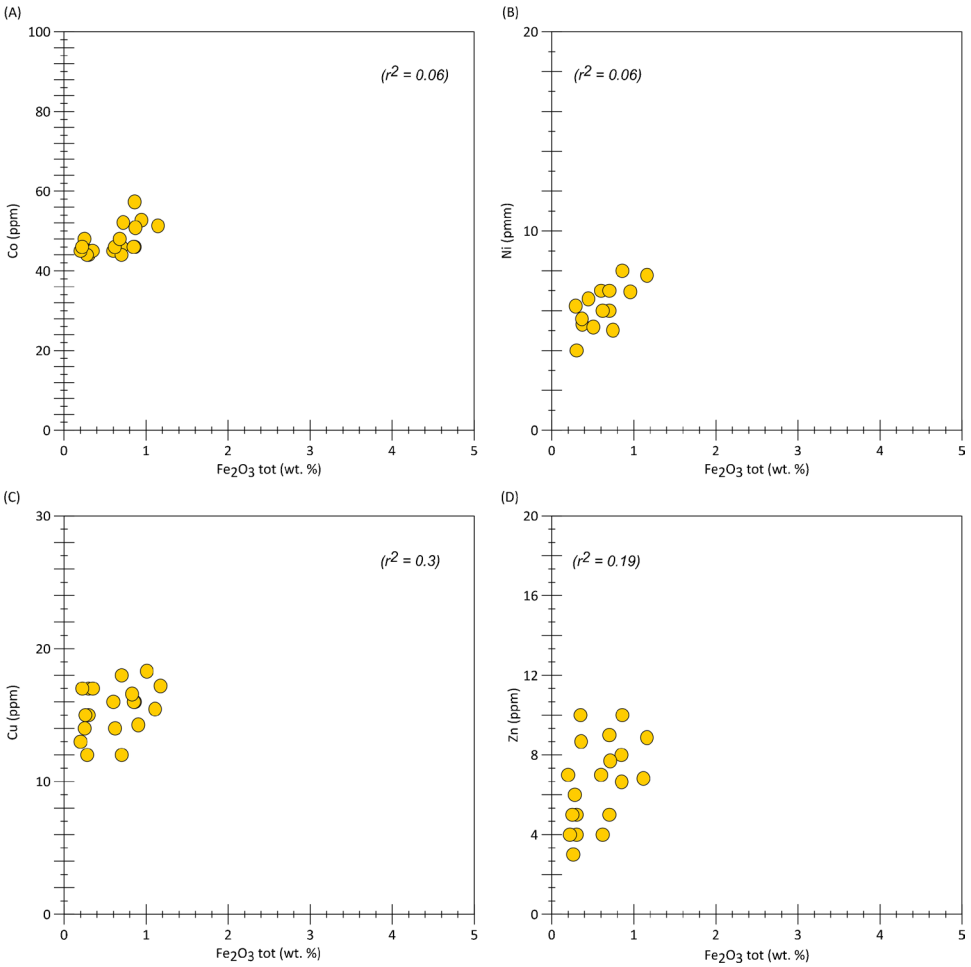

Fig. 8 **A**–**D** Correlation diagrams of Fe_2O_3tot with Co, Ni, Cu, and Zn

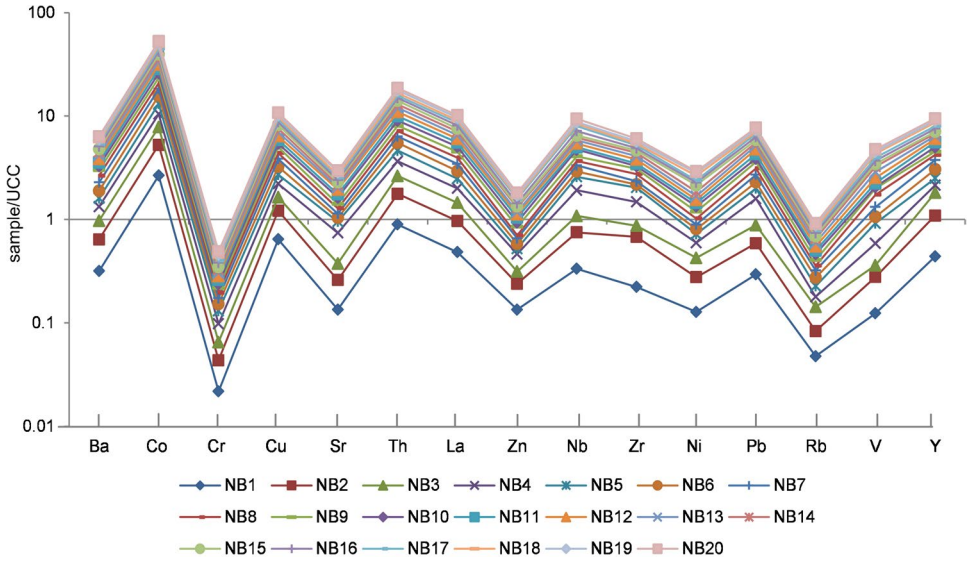

Fig. 9 A UCC-normalized multi-element diagram for the studied sandstones. Average normalized values derived from Rudnick and Gao (2003)

for the studied sandstone samples (Fig. 12A–D). Plotting of the studied samples on the ternary Ni-V-Th*10 diagram of Bracciali et al. (2007) and on the bivariate Ni versus TiO_2 diagram of Floyd et al. (1989) indicates a felsic source for the studied sandstones (Fig. 13A, B).

The studied sandstones show high Ba and Co concentrations, and the high Ba/Co ratio confirms the derivation from a weathered intermediate igneous provenance (Cullers et al. 1988; McLennan et al. 1993; Cullers 2000; Akarish and El-Gohary 2008; Löwen et al. 2018). Trace element values given in Table 3 show that the studied sandstones are rich in Ba, Th, and Sr, while exhibit depletion in transitional elements (e.g., Cr, Ni, and V). Notable negative anomalies of Cr, Rb, Sr, and Ba (see Fig. 9) are most probably attributed to the remarkable paucity of feldspars. On the other hand, high positive anomalies of Co, Zr, and Nb suggest prevailing felsic than mafic provenance. The low concentrations of Cr and Ni may suggest a mafic provenance, and the minerals containing these elements (e.g., pyroxenes) were broken down over time as a result of chemical and physical weathering (Zhang et al. 1998; Osae et al. 2006; Akarish and El-Gohary 2008). Relatively high concentration of Zr indicates increasing of heavy minerals, especially zircon and garnet.

Tectonic control of deposition

The results of the undertaken petrographic examination imply that the studied sandstones are distinguished by high content of quartz, predominance of monocrystalline quartz, and scarcity of feldspars and lithic fragments. These characteristics are consistent largely with deposition in the continental craton interior basins (Crook 1974; Potter 1978; Taylor and McLennan 1985). Additionally, plotting detrital mode data of the analyzed samples on the QFL ternary diagram of Dickinson et al. (1983) suggests that the Nubian sandstones are mainly of cratonic interior and quartzose

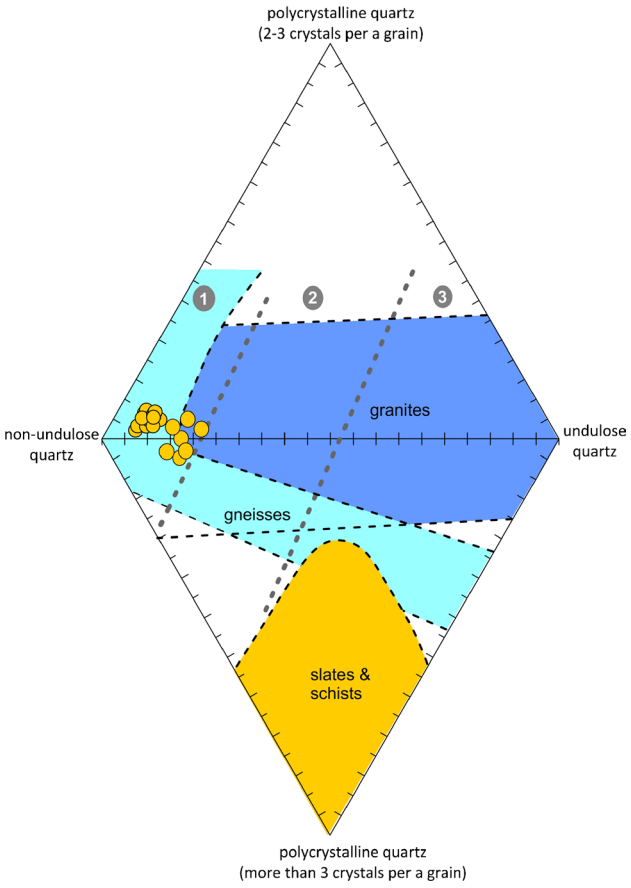

Fig. 10 Point-count data of the studied Nubian sandstones plotted on the diagram of Tortosa et al. (1991) for provenance discrimination

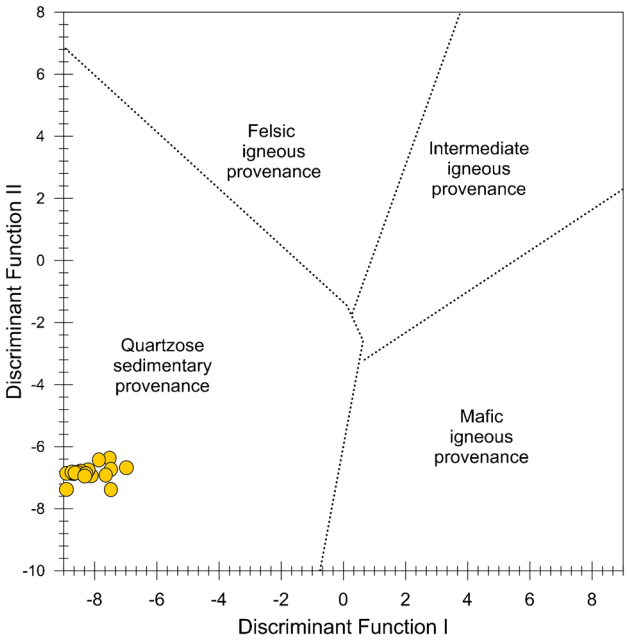

Fig. 11 Provenance of the studied sandstones based on discriminant function diagram of Roser and Korsch (1988)

recycled orogenic tectonic provenances (Fig. 14) (cf. Taylor and McLennan 1985; Ahfaf et al. 2021).

Percentages of quartz in the sandstones can also be used to recognize their tectonic settings. According to Crook's classification (1974), the studied sandstones are quartz-rich (average 92.26%); thus, they are consistent chiefly with the sandstones of the Atlantic-type (i.e., passive margin).

Plotting of the major element values on the ternary and bivariate diagrams of Bhatia (1983), Roser and Korsch (1986), Kroonenberg (1994), and Verma and Armstrong-Altrin (2016) (Figs. 15A–C and 16A, B) ascertains that the studied sandstones were deposited mainly in the passive continental margin. Plotting trace element values on the logarithmic function diagrams after Verma and Armstrong-Altrin (2016) (Fig. 17A, B) implies a passive continental margin setting of the studied sandstones. The employment of the function diagram of Verma and Armstrong-Altrin et al. (2013) implies that the studied sandstones are attributed to continental rift setting (Fig. 17C).

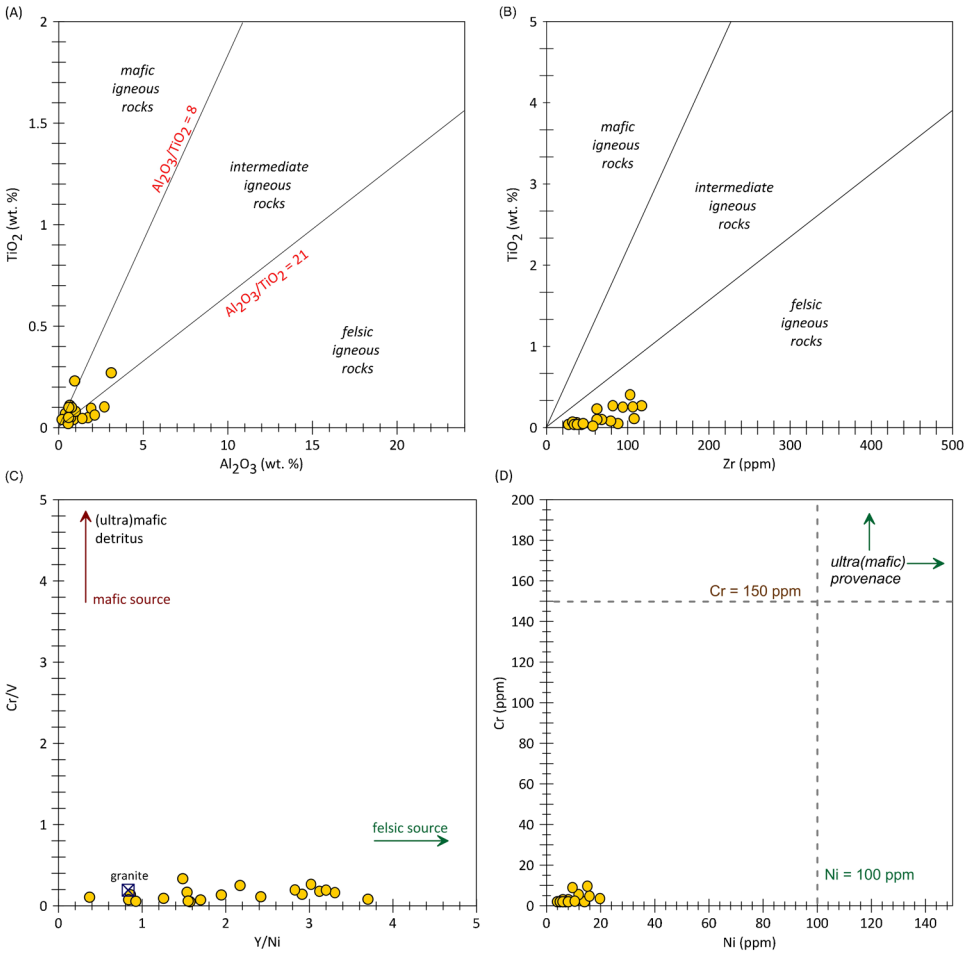

Fig. 12 Bivariate plot diagrams showing the provenance of the studied Nubian sandstones: **A** Al_2O_3 versus TiO_2 diagram (after Hayashi et al. 1997), **B** Zr versus TiO2 cross plot diagram (after Hayashi et al. 1997), **C** Cr/V versus Y/Ni cross plot (after Hiscott 1984), and **D** Ni versus Cr diagram (after Garver et al. 1996)

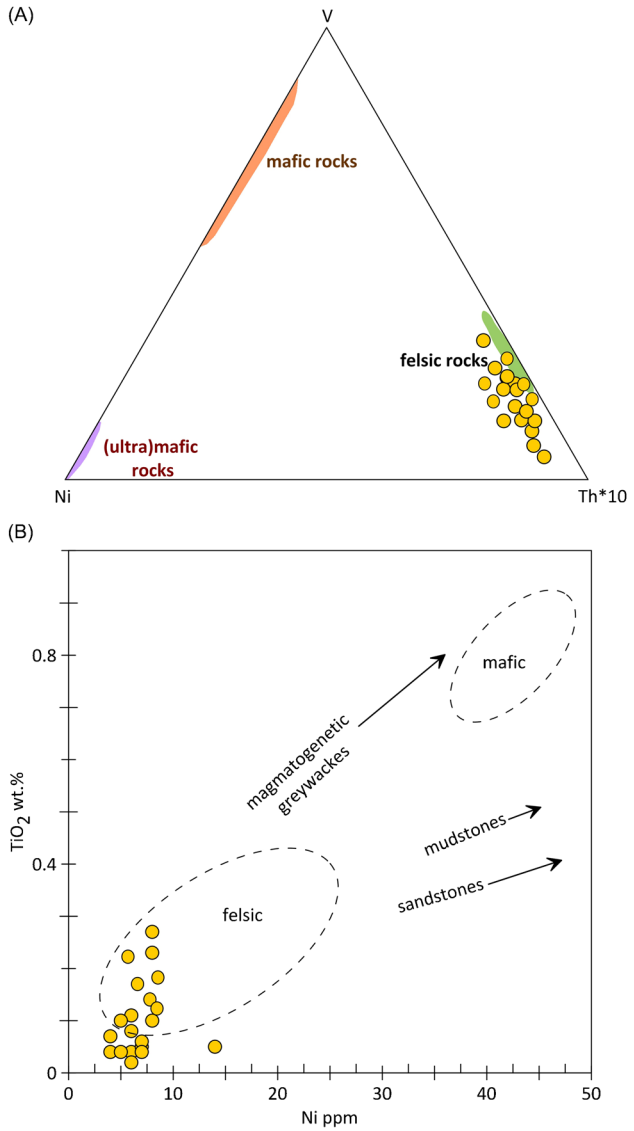

Fig. 13 **A** Plots of the studied sandstone samples on the Ni–V–Th*10 ternary diagram after Bracciali et al. (2007) and **B** Ni/TiO_2 bivariate diagram of Floyd et al. (1989) used for provenance determination of the analyzed sandstone samples

Source area palaeoweathering and palaeoclimate

In the studied sandstones, the high proportions of monocrystalline quartz (average 94.85% of the total quartz), less amount of polycrystalline quartz grains (average 5.41% of the total quartz), as well as the very scarcity of feldspar minerals (average 1.17%) (Table 1) indicate a prolonged chemical palaeoweathering of the source rocks and several phases of recycling (Dabbagh and Rogers 1983; Wanas and Abdel-Maguid 2006; Al-Habri and Khan 2008).

The calculated CIA and CIW values for the studied sandstone samples range from 86.23 to 99.46 (average 96.30) and 87.31 to 99.73 (average 97.62), respectively (Table 2). These high values of the CIA and CIW indicate intensive weathering and reflect warm humid climatic conditions in the source rock area. The CIA values for the studied sandstones are plotted in the Al_2O_3 - (CaO* + Na_2O) - K_2O ternary diagram after Nesbitt and Young (1982) (Fig. 18A). The highest degree of alteration (CIA) points to felsic-granitic source. As indicated in Table 2, the high values of the CIA and CIW are attributed mainly to the depletion of mobile elements (e.g., Ca, Na, and K) relative to the less mobile and residual elements (Al and Ti) (Nesbitt and Young 1982). On the ternary Al_2O_3-Zr-TiO_2 diagram of Garcia et al. (1991), the analyzed sandstone samples display high Zr and relatively low Al_2O_3 and TiO_2 (Fig. 18B) indicating an increasing of sorting (Nesbitt et al. 1996). The bivariate plot of SiO_2 versus total $Al_2O_3 + K_2O + Na_2O$ proposed by Suttner and Dutta (1986) was used to identify the chemical maturity of the Nubia sandstones as a function of climate. This plot reveals the increasing of chemical maturity of the studied sandstones under humid and semi-humid climatic conditions in the source area (Fig. 18C).

Palaeogeographical interpretation

The usage of various interpretative approaches based on geochemical and petrographic data permits making a series of the relevant interpretations. Additionally, the position of the samples of the sandstones is illustrated on several provenance-related diagrams (Figs. 5, 6, 7, 8, 9, 10, 11, 12, 13, 14, 15, 16, 17 and 18). Generally, these interpretations imply that the sandstones were sourced mainly from an older quartzose sedimentary provenance.

In southern Egypt, thick Paleozoic successions are well developed in three sedimentary basins, namely, Uweinat–Gilf, South Nile Valley, and Etbai (Issawi et al. 2016; Issawi and Sallam 2018). The Paleozoic rocks in these basins consist mainly of fluvial and glacial sediments (mostly sandstones and conglomerates). These sediments were classified into the Araba Fm. (Cambrian) at the base, followed upward by the Gabgaba Fm. (Ordovician), Naqus Fm. (Silurian), Wadi Malik Fm. (Devonian), Gilf Fm. (Carboniferous), and Abu Ras Fm. (Permo-Triassic) (Osman et al. 2003, 2005; Issawi and Sallam 2018). These lithostratigraphic units unconformably overlie the Precambrian basement rocks (Klitzsch 1981; Garfunkel 1999, 2002). It is apparently that the Paleozoic sediments in these basins were derived mostly from intense denudation, disintegration, and erosion of the surrounding Precambrian rocks of the Arabo–Nubian Shield and Gebel Uweinat located in southwestern Egypt (Fig. 19). During the Early Cretaceous,

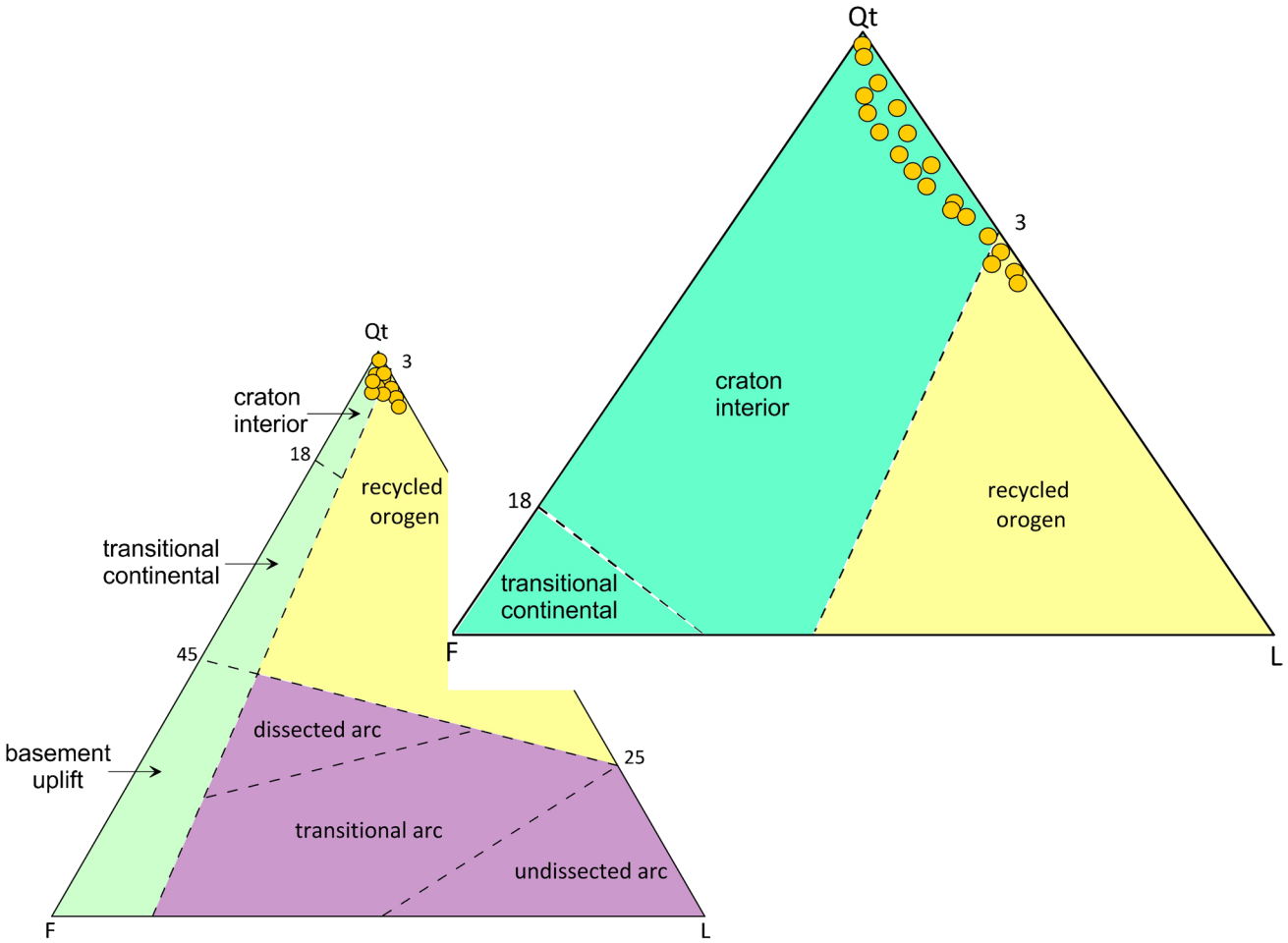

Fig. 14 Ternary plot diagram of detrital components of the studied sandstones on the tectonic provenance discrimination diagram of Dickinson et al. (1983). Abbreviations: Q, total quartz; F, feldspars; L, lithic fragments

multiple cycles of erosion and sedimentation took place (Kolodner et al. 2006), and the Paleozoic rocks were eroded and recycled repeatedly by ancient fluvial streams flowed in poly-directional patterns. This recycling process led to the formation of thick sheets of younger matured cross-bedded sandstones in low-lying basinal areas in the passive continental margin in southern and southeastern Egypt (Fig. 19). In Libya, the country bordering Egypt from the west, Ahfaf et al. (2021) documented a predominant plutonic provenance with some metamorphic supply for the Upper Sarir quartzose sandstones in the Sirt Basin, which are coeval with the Nubian sandstones in southern Egypt and northern Sudan. They also indicated that the Sarir sandstones were formed from a cratonic basement in humid palaeoclimatic environments accompanied by a rigorous chemical palaeoweathering in the source area. These conditions probably produced similar Lower Cretaceous quartzose sandstones in other territories in north and north-eastern Gondwana (Ahfaf et al. 2021). On the other side, in Palestine/Israel which border Egypt from the northeast, Kolodner et al. (2009) attributed the origin of the Lower Cretaceous Nubian sandstones cropping out in the Negev Desert to recycling of relatively proximal Paleozoic sandstones, using U-Pb Sensitive High Resolution Ion Micro-Probe (SHRIMP) dating of detrital zircon from these sandstones. From the foregoing discussion, it is concluded that the studied Nubian sandstones were partly produced by fluvial recycling from Paleozoic sandstones in the proximal surrounding basins, with a considerable contribution of basement denudation. This interpretation is consistent and in agreement with the conclusion of Shawa and Issawi (1978) that attributed the source area of the Nubian sandstones to an exposed landmass located in southeastern and southern Egypt. This provenance patterns need to be brought in correspondence to the palaeogeographical reconstructions of northeastern Africa in the Early Cretaceous in regard to the palaeolocation of the study area.

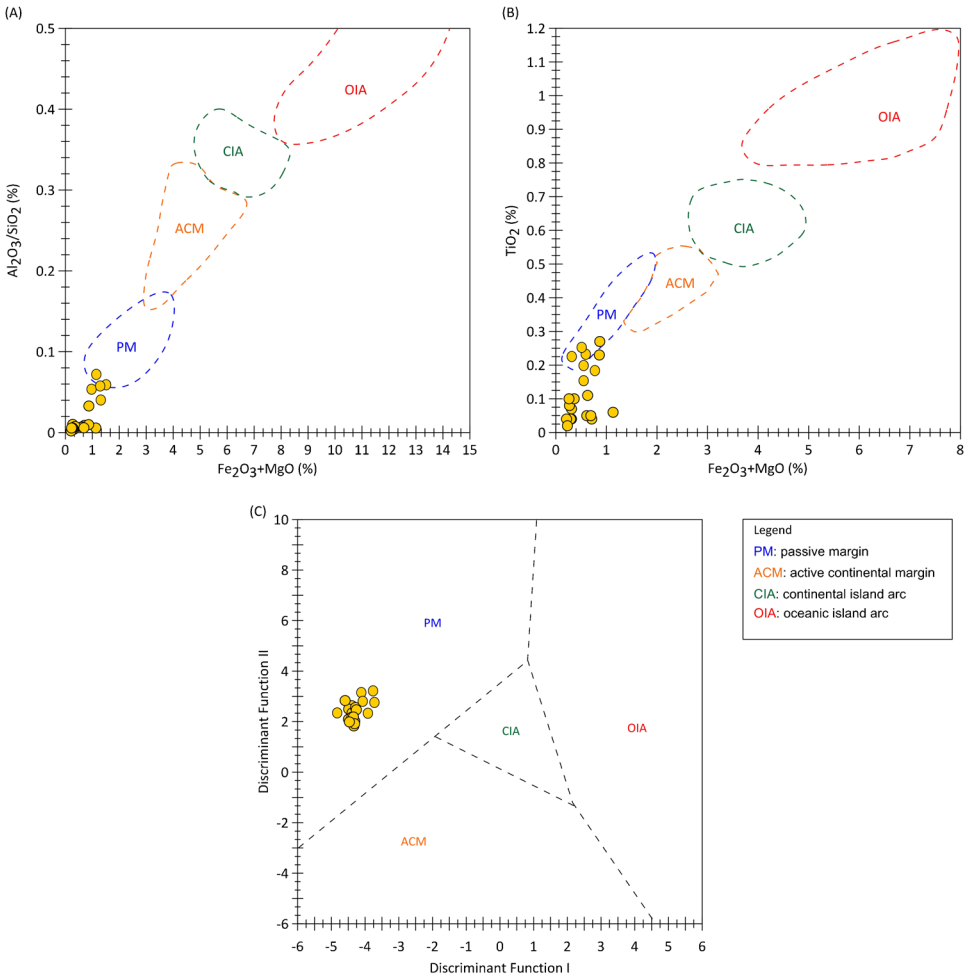

Fig. 15 Plots of the major element composition of the studied sandstones on the discrimination diagrams for tectonic setting (after Bhatia (1983))

According to Guiraud et al. (2001, 2005), the northeastern Africa was embraced by a large epeiric sea in the Cretaceous (Fig. 19). Since the Early Cretaceous, this sea penetrated from the north, i.e., it was a marginal sea of the Eastern Mediterranean (Golonka 2004). The southern edge of the noted epeiric sea reached the southern part of modern Egypt, and it was controlled by a W–E-trending fault system with strike-slip displacements (Guiraud et al. 2005). The land corresponded to the African–Arabian continental landmass, with lowlands dominated by alluvial and lacustrine plains and denudated uplands located not so far from the coastline; the study area was located at the very land–sea transition (Fig. 19). More generally, the Nubia Formation exposed at Gebel Duwi represents a wide intracontinental zone marking a transition between the interiors (denudated land) and the periphery (epeiric sea) of a very large continent. The

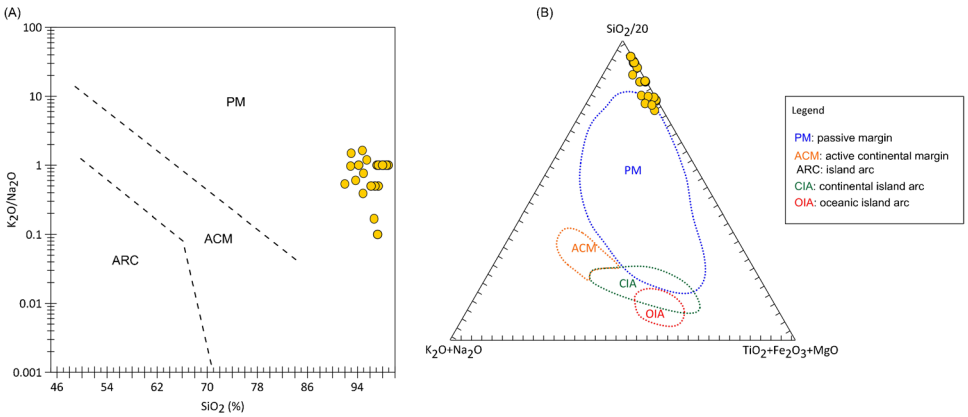

Fig. 16 Plots of the major element composition of the studied sandstones on the discrimination diagram for tectonic setting: **A** after Roser and Korsch (1986) and **B** after Kroonenberg (1994)

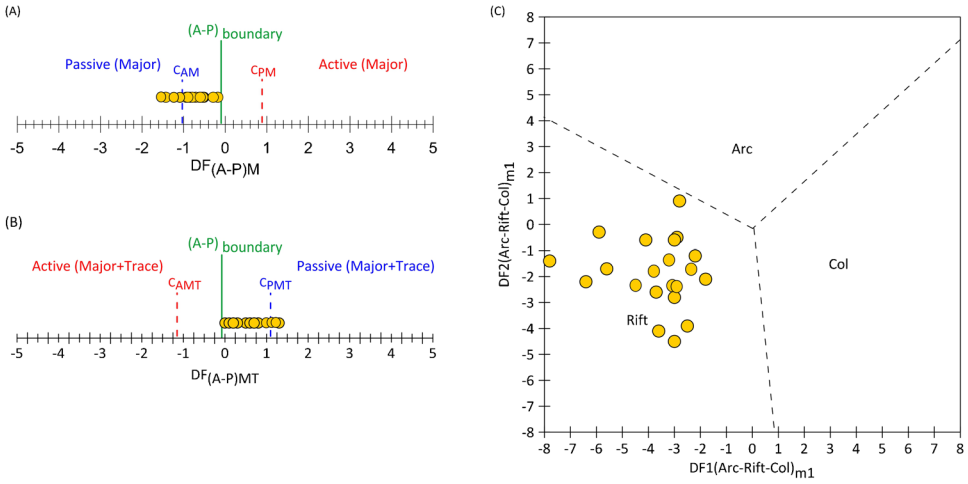

Fig. 17 Tectonic setting discrimination of the Nubian sandstones. **A** Multi-dimensional discriminant function diagram for the discrimination of tectonic settings after Verma and Armstrong-Altrin et al. (2013). Multi-dimensional discriminant function diagrams for the discrimination of active and passive margin settings after Verma and Armstrong-Altrin (2016): **B** using major elements and **C** using both major and trace elements. Abbreviations: Arc, island or continental arc; Rift, continental rift; Col, collision

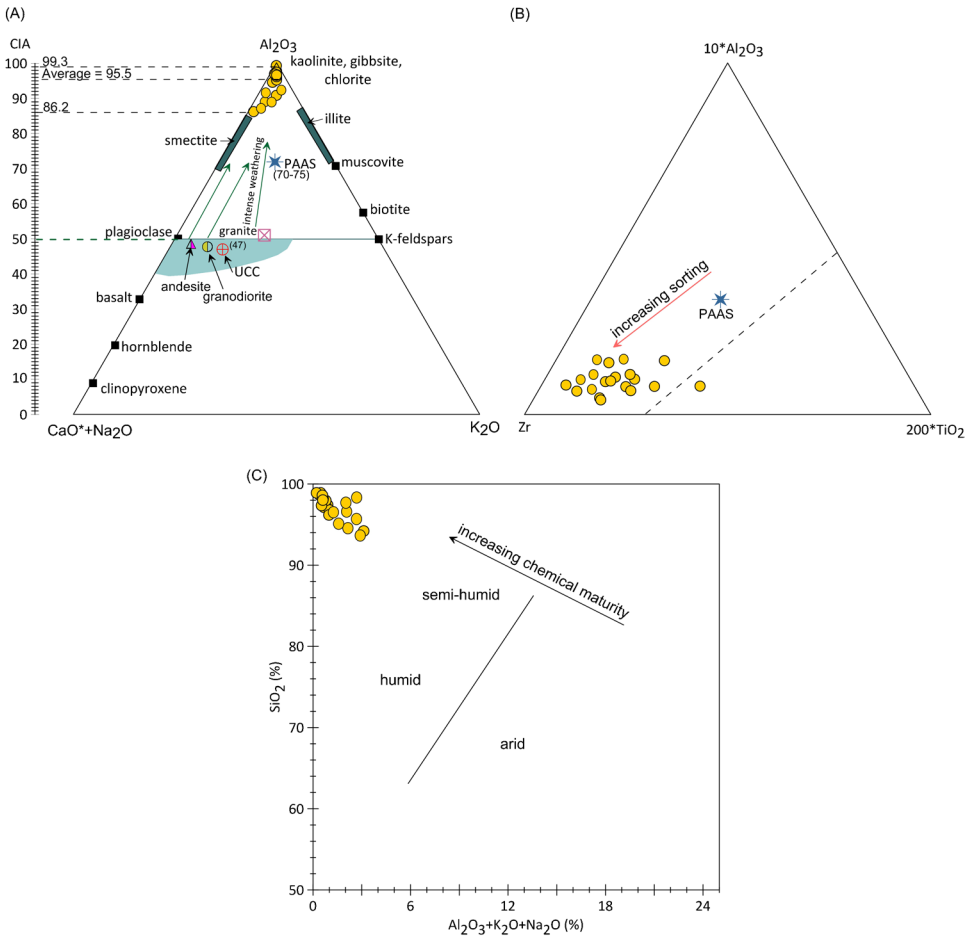

Fig. 18 **A** Ternary Al_2O_3–CaO^*+Na_2O–K_2O plot diagram for the studied sandstones (after Nesbitt and Young 1982). CaO^* is the molar proportion of CaO in the silicate fraction; and CIA is the Chemical Index of Alteration; **B** Al_2O_3–Zr–TiO_2 ternary diagram showing the influence of sorting process (after Garcia et al. 1991) and **C** binary plot diagram of SiO_2 versus ($Al_2O_3+K_2O+Na_2O$) for the determination of the climatic conditions during the deposition of the studied sandstones (after Suttner and Dutta (1986))

composition of the studied sandstones at Gebel Duwi reveals its fluvial origin, which corresponds well to the existence of the alluvial plain. Deltaic origin of the upper lithofacies of the Nubia Formation and its gradual transition to the shallow-marine deposits of the overlying Quseir Formation imply long-term transgression that is also well-documented by the regional-scale palaeogeographical reconstructions (Guiraud et al. 2005; An et al. 2017). Moreover, it is evident that the lower and middle lithofacies of the Nubia Formation were deposited on the alluvial plain, but not so far from the coastline, as the lithofacies change occurred already during the deposition of this formation.

The provenance patterns revealed by the present study are in agreement with the palaeogeographical reconstructions

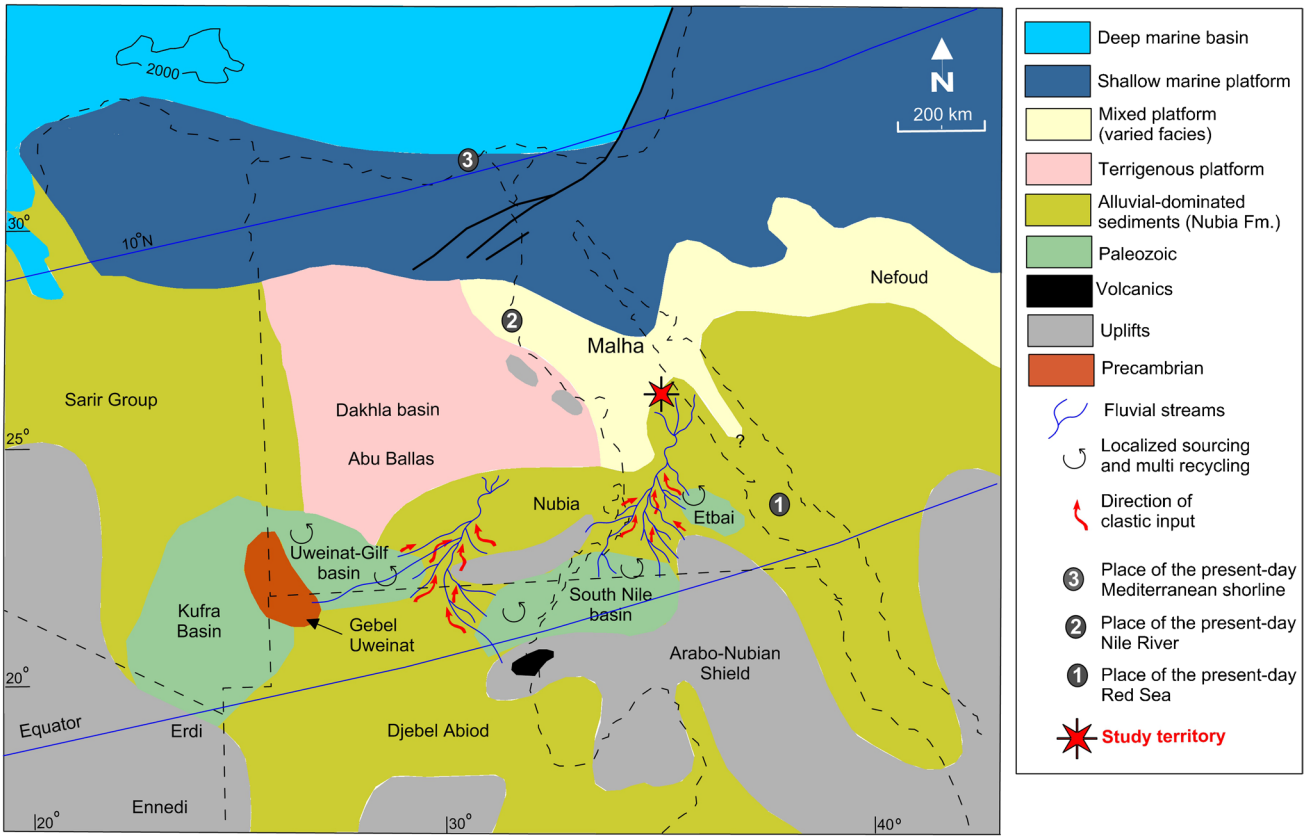

Fig. 19 Early Cretaceous palaeogeographical map (modified after Guiraud et al. (2001))

(Guiraud et al. 2001, 2005; Wanas and Assal 2021). The detrital material was denudated from the uplifts of the continental interiors. Most probably, these were the uplifts of modern southeastern part of Egypt. However, the spatial orientation of lowlands and uplifts (Fig. 19) allows hypothesizing delivery of some material also from the Arabo-Nubian Shield. Two questions are about the tectonic setting and the palaeoclimate. The results of the present study indicate on a stable tectonic regime. However, the Cretaceous fault activity, volcanism, and rather rapid changes in configuration of the principal palaeogeographical elements (Guiraud et al. 2005) imply that it was not so stable. This controversy should be explained in the terms of insufficient resolution of the provenance-related interpretation techniques for making clear distinction between fully stable and tectonically active regimes of the continental interiors. As for the climate, it appears that it was humid in the source rock areas, i.e., in the denudated uplifts. The relatively close position of the latter to the study area implies that humid conditions could be typical to the alluvial plain too. This is in agreement with some other interpretations (e.g., Selim 2017). However, Beauchamp et al. (1990) noted earlier the dry depositional environments of the sandstones, and Klitzsch (1990) suggested regional climate changes. So, the open question for further investigations is whether the Lower Cretaceous sandstones at Gebel Duwi reflects the accumulation of the entire Nubia Formation in humid conditions or these sandstones deposited during any humid episode.

Although the precise age of the Nubia Formation remains debatable (e.g., Bosworth et al. in Hamimi et al. 2020), this does not challenge the proposed palaeogeographical interpretations in regard to the persistence of more or less the same conditions through the Cretaceous (Guiraud et al. 2001; Wanas and Assal 2021). It is worth to add that the provenance-related interpretations for the Lower Cretaceous sandstones exposed at Gebel Duwi in the Quseir area resemble the outcomes of the previous study of the Middle Jurassic sandstones in the Khashm El-Galala area (Sallam and Wanas 2019). Probably, there were universal patterns of the mechanisms of crystalline basement denudation and fluvial sandstone formation at the long-existed continental interiors–periphery transition of northeastern Africa.

Conclusions

The studied Nubian sandstones at Gebel Duwi (Quseir area, Eastern Desert) are quartzose and litho-quartzose that are enriched in SiO_2 and Ba, Co, Th, Zr, and Sr. These sandstones were deposited on an alluvial plain, and they

were partly formed through multiple stages of fluvial recycling from Paleozoic siliciclastic rocks, with a considerable contribution of basement denudation in a humid environment, which certainly favored intense chemical and physical weathering. The enriched ZTR (zircon + tourmaline + rutile) content and paucity of feldspars confirm an increasing proportion of detritus recycled from older siliciclastic units. The compositional and provenance features of these sandstones characterize the very transition from the interiors of a large continent and its periphery.

Supplementary Information The online version contains supplementary material available at https://doi.org/10.1007/s12517-021-08743-3.

Acknowledgements The authors gratefully thank the journal editor and the reviewer for their helpful suggestions and M. Mogahed (Benha University, Egypt) for his help in drawing plot diagrams.

Author contribution Field investigations, laboratory analysis, and data acquisition were performed by E.S. Sallam. Data interpretation and discussion have been written by E.S. Sallam and D.A. Ruban.

Declarations

Conflict of interest The authors declare no competing interests.

References

Abd El-Razik TM (1967) Stratigraphy of the sedimentary cover of the Anz-Atshan-south Duwi district. Bull Fac Sci Cairo University 431:135–179

Ahfaf MMA, Adepehin EJ, Che Aziz Ali CA, Jamil H, Sylvester Powei Lubi SP (2021) Controls on the compositional framework and petrogenesis of Early Cretaceous first cycle quartzose sandstone, North Gondwana. Sediment Geol 424:105982

Akaad MK, Noweir AM (1980) Geology and lithostratigraphy of the Arabian desert orogenic belt between latitudes 25^0 35′ and 26^0 30′. In: Cooray PATS (ed) Evolution and Mineralization of the Arabian-Nubian shield. Permagon Press, New York, pp 127–135

Akarish AM, El-Gohary AM (2008) Petrography and geochemistry of lower Paleozoic sandstones, East Sinai, Egypt: implications for provenance and tectonic setting. J Afr Earth Sci 52:43–54

Akinlotan OO, Adepehin EJ, Rogers GH, Drumm EC (2021) Provenance, palaeoclimate and palaeoenvironments of a non-marine Lower Cretaceous facies: petrographic evidence from the Wealden Succession. Sediment Geol 415:105848

Al-Habri OA, Khan MM (2008) Provenance, diagenesis, tectonic setting and geochemistry of Tawil sandstone (Lower Devonian in central Saudi Arabia). J Asia Earth Sci 33:278–287

Amireh BS (1991) Mineral composition of the Cambrian-Cretaceous Nubian series of Jordan: provenance, tectonic setting and climatological implications. Sediment Geol 71:99–119

An K, Chen H, Lin X, Wang F, Yang S, Wen Z, Wang Z, Zhang G, Tong X (2017) Major transgression during Late Cretaceous constrained by basin sediments in northern Africa: implication for global rise in sea level. Front Earth Sci 11:740–750

Armstrong-Altrin JS, Nagarajan R, Madhavaraju J, Rosalez-Hoz L, Lee YI, Balaram V, Cruz-Martinez A, Avila-Ramirez G (2013) Geochemistry of the Jurassic and upper Cretaceous shales from the Molango Region, Hidalgo, Eastern Mexico: implications of source area weathering, provenance, and tectonic setting. C R Geosci 345:185–202

Basu A, Young S, Suttner L, James W, Mack G (1975) Re-evaluation of the use of undulatory extinction and crystallinity in detrital quartz for provenance interpretation. J Sediment Petrol 45:873–882

Beauchamp J, Omer MK, Perriaux J (1990) Provence and dispersal of Cretaceous elastics in northeastern Africa: climatic and structural setting. J Afr Earth Sci 10:243–251

Bhatia MR (1983) Plate tectonics and geochemical composition of sandstones. J Geol 91:611–627

Bhatia MR, Crook KW (1986) Trace element characteristics of greywackes and tectonic setting discrimination of sedimentary basins. Contrib Mineral Petrol 92:181–193

Bracciali L, Marroni M, Pandolfi L, Rocchi S (2007) Geochemistry and petrography of Western Tethys Cretaceous sedimentary covers (Corsica and Northern Apennines): from source areas to configuration of margins. In: Arribas J, Critelli S, Johnsson MJ (Eds.), Sedimentary provenance and petrogenesis: perspectives from petrography and geochemistry. vol. 420. The Geological Society of America, Special Paper, pp 73–93

Crook KAW (1974) Lithostratigraphy and geotectonic: the significance of composition variation in flyscharenites (graywakes). In: Dott RH, Shaver RH (Eds.), Modern and Ancient Geosynclinal Sedimentation. vol. 19. Society of Economic Palaeontologists and Mineralogists, special publication, pp 304–310

Cullers RL (2000) The geochemistry of shales, siltstones and sandstones of Pennsylvanian–Permian age, Colorado, U.S.A.: implications for provenance and metamorphic studies. Lithos 51:181–203

Cullers R, Basu A, Suttner LJ (1988) Geochemical signature of provenance in sand-sized material in soil and stream sediments near the Tobacco Root Batholith, Montana, USA. Chem Geol 70:335–348

Dabbagh ME, Rogers JJ (1983) Depositional environments and tectonic significance of the Wajid Sandstone of southern Saudi Arabia. J Afr Earth Sci 1:47–57

Dickinson WR, Suczek CA (1979) Plate tectonics and sandstone compositions. Am Assoc Pet Geol 63:2164–2182

Dickinson WR, Beard LS, Brakenridge GR, Erjavec JL, Ferguson RC, Inman KF, Knepp RA, Lindberg FA, Ryberg PT (1983) Provenance of North American Phanerozoic sandstones in relation to tectonic setting. Geol Soc Am Bull 94:222–235

Dinis PA, Garzanti E, Hahn A, Vermeesch P, Cabral-Pinto M (2020) Weathering indices as climate proxies. A step forward based on Congo and SW African river muds. Earth Sci Rev 201:103039

Floyd PA, Franke W, Shail R, Dorr W (1989) Geochemistry and tectonic setting of Lewisian clastic metasediments from the Early Proterozoic Loch Maree Group of Gairloch, NW Scotland. Precambrian Res 45:203–214

Folk RL (1974) Petrology of Sedimentary Rocks: Austin. Hemphill, Texas, p 182

Garcia D, Coelho J, Perrin M (1991) Fractionation between TiO2 and Zr as a measure of sorting within shale and sandstone series (northern Portugal). Eur J Mineral 3:401–414

Garfunkel Z (1999) History and paleogeography during the Pan-African orogen to stable platform transition: reappraisal of the evidence from Elat area and the northern Arabian-Nubian Shield. Isr J Earth Sci 48:135–157

Garfunkel Z (2002) Early Palaeozoic sediments of NE Africa and Arabia: products of continental-scale erosion, sediment transport, and deposition. Isr J Earth Sci 51:135–156

Garver JI, Royce PR, Smick TA (1996) Chromium and nickel in shale of the Taconic foreland: a case study for the provenance

of fine-grained sediments with an ultramafic source. J Sediment Res 66:100–106
Garzanti E (2016) From static to dynamic provenance analysis-sedimentary petrology upgraded. Sediment Geol 336:3–13
Garzanti E (2019) Petrographic classification of sand and sandstone. Earth Sci Rev 192:545–563
Garzanti E, Andò S (2019) Heavy minerals for junior woodchucks. Minerals 9:148
Garzanti E, Dinis P, Vermeesch P, Ando S, Hahn A, Huvi J, Limonta M, Padoan M, Resentini A, Rittner M, Vezzoli G (2018) Dynamic uplift, recycling, and climate control on the petrology of passive-margin sand (Angola). Sediment Geol 375:86–104
Golonka J (2004) Plate tectonic evolution of the southern margin of Eurasia in the Mesozoic and Cenozoic. Tectonophysics 381:235–273
Guiraud R, Issawi B, Bosworth W (2001) Phanerozoic history of Egypt and surrounding areas. In: Ziegler PA, Cavazza W, Robertson AHF, Crasqun-Soleau S (Eds.), Peri-Tethys Memoir 6: Peri-Tethyan Rift/Wrench Basins and Passive Margins. vol. 186. Mém. Mus. natn. Hist. nat., pp 469–509
Guiraud R, Bosworth W, Thierry J, Delplanque A (2005) Phanerozoic geological evolution of Northern and Central Africa: an overview. J Afr Earth Sci 43:83–143
Hamimi Z, El-Barkooky A, Martinez Frias J, Fritz H, El-Rahman Y (2020) The Geology of Egypt. Springer, Cham, p 711
Harnois L (1988) The CIW index: a new chemical index of weathering. Sediment Geol 55:319–322
Haughton PDW, Todd SP, Morton AC (1991) Sedimentary provenance studies. In: Geological Society, 57th edn. Special Publication, London, pp 1–11
Hayashi K, Fujisawa H, Holland H, Ohmoto H (1997) Geochemistry of ~1.9 Ga sedimentary rocks from northeastern Labrador, Canada. Geochim Cosmochim Acta 61:4115–4137
He J, Wang H, Garzanti E (2020) Petrographic analysis and classification of sand and sandstone. Earth Sci - J China Univ Geosci 45:2186–2198
Heath R, Vanstone S, Swallow J, Ayyad M, Amin M, Huggins P, Swift R, Warburton I, McClay K, Younnis A (1999) Renewed exploration in the offshore north Red Sea Region, Egypt. In: Proceedings of the 14th Petroleum Conference. Egyptian General Petroleum Corporation, Cairo, pp 16–34
Hindrix MS (2000) Evaluation of Mesozoic sandstone composition, southern Junggar, northern Tarim and western Turran basins, northwest China: a detrital record of the ancestral Tian Shan. J Sediment Res 70:520–532
Hiscott R (1984) Ophiolitic source rocks for Taconic-Age flysch: trace-element evidence. Geol Soc Am Bull 95:1261–1267
Ingersoll RV, Suczek CA (1979) Petrology and provenance of Neogene sand from Nicobarand Bengal fans, DSDP sites 211 and 218. J Sediment Petrol 49:1217–1228
Ingersoll RV, Bullard T, Ford R, Grimm J, Pickle J, Sares S (1984) The effect of grain size on detrital modes: a test of the Gazzi Dickinson point-counting method. J Sediment Petrol 54:103–116
Issawi B, Sallam ES (2018) Stratigraphy and facies development of the pre-Cenozoic sediments in southern Egypt: a geodynamic approach. Arab J Geosci 11:271
Issawi B, Ahmed SM, Osman R, Sallam ES (2005) Studies on the Pliocene—Quaternary sediments in the western fringes of the Nile Delta—lower Nile Valley stretch, Egypt. Sedimentology Egypt 13:277–296
Issawi B, Sallam E, Zaki SR (2016) Lithostratigraphic and sedimentary evolution of the Kom Ombo (Garara) sub-basin, southern Egypt. Arab J Geosci 9:420
Khalil SM, McClay KR (2009) Structural control on syn-rift sedimentation, northwestern Red Sea margin, Egypt. Mar Pet Geol 26:1018–1034
Klitzsch E (1981) Lower Palaeozoic rocks of Libya, Egypt and Sudan. In: Holland CH (ed) Lower Palaeozoic Rocks of the Middle East, Eastern and Southern Africa and Antarctica. Wiley, London, pp 131–163
Klitzsch E (1990) Paleogeographical development and correlation of Continental Strata (former Nubian Sandstone) in northeast Africa. J Afr Earth Sci 10:199–213
Kolodner K, Avigad D, Mcwilliams M, Wooden JL, Weissbrod T, Feinstein S (2006) Provenance of north Gondwana Cambrian-Ordovician sandstone: U-Pb SHRIMP dating of detrital zircons from Israel and Jordan. Geol Mag 143:367–391
Kolodner K, Avigad D, Ireland TR, Garfunkel Z (2009) Origin of Lower Cretaceous ('Nubian') sandstones of North-east Africa and Arabia from detrital zircon U-Pb SHRIMP dating. Sedimentology 56:2010–2023
Kröner A (1984) Late Precambrian plate tectonics and orogeny: a need to redefine the term Pan-African. In: Klerkx J, Michot J (eds) African Geology. Musée. R. l'Afrique Centrale, Tervuren, pp 23–28
Kröner A (1993) The Pan African belt of northeastern and Eastern Africa, Madagascar, southern India, Sri Lanka and East Antarctica: terrane amalgamation during the formation of the Gondwana supercontinent. In: Thorweihe U, Schandelmeier H (eds) Geoscientific Research in Northeast Africa. Balkema, Rotterdam, pp 3–9
Kroonenberg SB (1994) Effects of provenance, sorting and weathering on the geochemistry of fluvial sands from different tectonic and climatic environments. Proceedings of the 29th International Geological Congress, Part A, pp 69–81
Löwen K, Meinhold G, Güngör T (2018) Provenance and tectonic setting of Carboniferous–Triassic sandstones from the Karaburun Peninsula, western Turkey: a multi-method approach with implications for the Palaeotethys evolution. Sediment Geol 375:232–255
McLennan SM, Hemming S, McDaniel DK, Hanson GN (1993) Geochemical approaches to sedimentation, provenance, and tectonics. In: Johnsson MJ, Basu A (eds) Processes Controlling the Composition of Clastic Sediments, vol 284. The Geological Society of America, Special Paper, Boulder, pp 21–40
Miall AD (1988) Facies architecture in clastic sedimentary basins. In: Kleinspehn KL, Paola C (eds) New Perspectives in Basin Analysis. Springer-Verlag, New York, pp 67–81
Middelburg JJ, van der Weijden CH, Woittiez JRW (1988) Chemical processes affecting the mobility of major, minor and trace elements during weathering of granitic rocks. Chem Geol 68:253–273
Mohammedyasin MS, Wudie G (2019) Provenance of the Cretaceous Debre Libanos Sandstone in the Blue Nile Basin, Ethiopia: Evidence from petrography and geochemistry. Sediment Geol 379:46–59
Morton AC (1985) Heavy minerals in provenance studies. In: Zuffa GG (ed) Provenance of Arenite. Reidel, Dordrecht
Morton AC, Hallsworth C (1994) Identifying provenance-specific features of detrital heavy mineral assemblages in sandstones. Sediment Geol 90:241–256
Nesbitt HW, Markovics G (1980) Chemical processes affecting alkalis and alkaline earths during continental weathering. Geochim Cosmochim Acta 44:1659–1666
Nesbitt HW, Young GM (1982) Early Proterozoic climates and plate motions inferred from major element chemistry of lutites. Nature 299:715–717
Nesbitt HW, Young GM, McLennan SM, Keays RR (1996) Effects of chemical weathering and sorting on the petrogenesis of

siliciclastic sediments, with implications for provenance studies. J Geol 104:525–542
Orszag-Sperber F, Purser BH, Rioual M, Plaziat JC (1998) Post Miocene sedimentation and rift dynamics in the southern Gulf of Suez and northern Red Sea. In: Purser BH, Bosence DWJ (eds) Sedimentation and Tectonics of Rift Basins: Red Sea-Gulf of Aden. Chapman and Hall, London, pp 427–447
Osae S, Asiedu DK, Yakubo B, Koeberl C, Dampare SB (2006) Provenance and tectonic setting of Late Proterozoic Buem sandstones of southeastern Ghana: evidence from geochemistry and detrital modes. J Afr Earth Sci 44:85–96
Osman R, Ahmed SM, Khater T (2003) The stratigraphy and facies of Wadi Gabgaba and its surroundings with an emphasis on the Lower Paleozoic glaciation. Sixth International Conference of the Arab World, Cairo Univ. Egypt 2:469–482
Osman R, Ahmed SM, Khater T (2005) Geological development of Wadi Gabgaba, Eastern Desert. Egypt. First International Conference on the Geology of Tethys, Cairo University 2:465–476
Philobbos ER, El Haddad AA, Luger P, Bekir R, Mahran T (1993) Syn-rift Miocene sedimentation around fault blocks in the Abu Ghusun-Wadi el Gemal area, Red Sea, Egypt. In: Philobbos ER, Purser BH (Eds.), Geodynamics and Sedimentation of the Red Sea-Gulf of Aden Rift System. The Geological Society of Egypt, Special Publication, vol. 1. pp 115–142
Potter PE (1978) Petrology and chemistry of modern Big River sands. J Geol 86:423–449
Roser BP, Korsch RJ (1986) Determination of tectonic setting of sandstone-mudstone suites using SiO_2 content and K_2O/Na_2O ratio. J Geol 94:635–650
Roser BP, Korsch RJ (1988) Provenance signature of sandstone-mudstone suite determined using discriminant function analysis of major element data. Chem Geol 67:119–139
Ruban DA, Sallam ES, Wanas HA (2019) Middle–Late Jurassic sedimentation and sea-level changes on the northeast African margin: a case study in the Khashm El-Galala area, NE Egypt. J Afr Earth Sci 156:189–202
Ruban DA, Sallam ES, Khater TM, Ermolaev VA (2021) Golden triangle geosites: preliminary geoheritage assessment in a geologically rich area of Eastern Egypt. Geoheritage 13(3):54
Rudnick RL, Gao S (2003) Composition of the continental crust. In: Holland HD, Turekian KK (Eds.), Treatise on Geochemistry. Elsevier-Pergamon, Oxford, vol. 3. pp. 1–64
Said R (1962) The geology of Egypt. Elsevier, Amsterdam and New York, p 377
Said R (1990) The geology of Egypt. Balkema, Rotterdam, p 734
Said R (2017) The geology of Egypt. Routledge, London, p 734
Sallam ES, Ruban DA (2020) Facies analysis and depositional environments of the Miocene syn-rift carbonate–siliciclastic rock packages in the northwest Gulf of Suez, Egypt. Carbonates Evaporites 35:10
Sallam ES, Wanas HA (2019) Petrography and geochemistry of the Jurassic siliciclastic rocks in the Khashm El-Galala area (NW Gulf of Suez, Egypt): implication for provenance, tectonic setting and source area paleoweathering. J Afr Earth Sci 160:103607
Sallam E, Wanas HA, Osman R (2015) Stratigraphy, facies analysis and sequence stratigraphy of the Eocene succession in the Shabrawet area (north Eastern Desert, Egypt): an example for a tectonically influenced inner ramp carbonate platform. Arab J Geosci 8(12):10433–10458
Sallam ES, Issawi B, Osman R, Ruban DA (2018) Deposition in a changing paleogulf: evidence from the Pliocene–Quaternary sedimentary succession of the Nile Delta, Egypt. Arab J Geosci 11:558
Selim SS (2017) Facies and sequence stratigraphy of fluvio-lacustrine deposits: Cretaceous Nubian succession of the Saharan platform (SW Egypt). Proc Geol Assoc 128:271–286
Shawa MS, Issawi B (1978) Depositional environments of the Nubia Sandstone, Upper Egypt. Ann Geol Surv Egypt 8:255–274
Stern RJ (1981) Petrogenesis and tectonic setting of Late Precambrian ensimatic volcanic rocks, Central Eastern Desert of Egypt. Precambrian Res 16:195–230
Stern RJ (1994) Arc assembly and continental collision in the Neoproterozoic East African orogen: implications for the consolidation of Gondwanaland. Annu Rev Earth Planet Sci 22:319–351
Stoeser DB, Camp VE (1985) Pan African microplate accretion of the Arabian shield. Geol Soc Am Bull 96:817–826
Suttner LJ, Dutta PK (1986) Alluvial sandstone composition and paleoclimate I. Framework mineralogy. J Sediment Res 56:329–345
Taylor SR, McLennan SM (1985) The continental crust: its composition and evolution. Blackwell Science Publisher, Oxford, p 312
Tortosa A, Palomares M, Arribas J (1991) Quartz grain types in Holocene deposits from the Spanish Central System: some problems in provenance analysis. In: Morton AC, Todd SP, Haughton PDW (Eds.), Developments in Sedimentary Provenance Studies. Geological Society of London, Special Publication, vol. 57. pp. 47–54
Van Houten FB, Bhattacharyya DP, Mansour SEJ (1984) Cretaceous Nubia Formation and correlative deposits, eastern Egypt: major regressive-transgressive complex. Geol Soc Am Bull 95:397–405
Verma SP, Armstrong-Altrin JS (2013) New multi-dimensional diagrams for tectonic discrimination of siliciclastic sediments and their application to Precambrian basins. Chem Geol 355:117–133
Verma SP, Armstrong-Altrin JS (2016) Geochemical discrimination of siliciclastic sediments from active and passive margin settings. Sediment Geol 332:1–12
Wanas HA, Abdel-Maguid NM (2006) Petrography and geochemistry of the Cambro-Ordovician Wajid Sandstone, southwest Saudi Arabia: implications for provenance and tectonic setting. J Asian Earth Sci 27:416–429
Wanas HA, Assal E (2021) Provenance, tectonic setting and source area-paleoweathering of sandstones of the Bahariya Formation in the Bahariya Oasis, Egypt: an implication to paleoclimate and paleogeography of the southern Neo-Tethys region during Early Cenomanian. Sediment Geol 413:105822
Wanas HA, Sallam E, Zobaa MK, Li X (2015) Mid-Eocene alluvial-lacustrine succession at Gebel El-Goza El-Hamra (Shabrawet area, NE Eastern Desert, Egypt): facies analysis, sequence stratigraphy and paleoclimatic implications. Sediment Geol 329:115–129
Ward WC, McDonald KC (1979) Nubia Formation of central Eastern Desert, Egypt – major subdivisions and depositional setting. Bull Am Assoc Pet Geol 63:975–983
Ward WC, McDonald KC, Mansour SEI (1979) The Nubia Formation of the Qusier – Safaga area, Egypt. Ann Geol Surv Egypt 9:420–431
Weissbrod T, Nachmias Y (1986) Stratigraphic significance of heavy minerals in the Late Precambrian-Mesozoic clastic sequence (Nubian Sandstone) in the near East. Sediment Geol 47:263–291
Youssef MI (1957) Upper Cretaceous rocks in Kosseir area. Bull de l'Inst du Desert d'Egypt 7:35–53
Zaid SM (2012) Provenance, diagenesis, tectonic setting and geochemistry of Rudies sandstone (Lower Miocene), Warda Field, Gulf of Suez, Egypt. J Afr Earth Sci 66-67:56–71
Zaid SM, Elbadry O, Ramadan F, Mohamed M (2015) Petrography and geochemistry of Pharaonic sandstone monuments in Tall San Al Hagr, Al Sharqiya Governorate, Egypt: implications for provenance and tectonic setting. Turk J Earth Sci 24:344–364
Zhang L, Sun M, Wang S, Yu X (1998) The composition of shales from the Ordos basin, China: effects of source weathering and diagenesis. Sediment Geol 116:129–141